


 Cite this: *RSC Adv.*, 2025, **15**, 12443

## Advanced clay-based geopolymers: influence of structural and material parameters on its performance and applications

 Rajwali Khan, <sup>\*a</sup> Shahid Iqbal, <sup>\*b</sup> Mukhlisa Soliyeva, <sup>c</sup> Ayaz Ali <sup>d</sup> and Noureddine Elboughdiri <sup>ef</sup>

Clay-based geopolymers are an intriguing alternative to traditional Portland cement when looking for ecologically friendly and sustainable building materials. This material blends cutting-edge geopolymers with abundantly available clay to produce a variety of advantages, including enhanced mechanical properties and reduced carbon emissions. As the need for green building solutions grows, clay-based geopolymers stand out because of their superior structural performance, durability, and resistance to extreme environmental conditions. In this study, we present a complete examination of the curing conditions, structural features, and diverse applications of geopolymers, emphasizing the essential elements that determine their strength and performance. We investigated the effect of curing temperature and duration, demonstrating that favorable curing temperatures (such as 60–80 °C) can increase the strength of geopolymers, whereas excessive curing temperatures can degrade their long-term structural integrity. Pre-curing treatments, such as heat and moisture management, were also investigated for their capacity to improve the microstructural density and minimize the porosity. In addition, we investigated improved curing procedures such as autoclave and steam-saturated methods, which provide higher mechanical qualities, especially in terms of compressive strength. Herein, we discussed a variety of applications, including high-performance composites in aerospace and construction and environmental remediation employing the capacity of geopolymers to immobilize dangerous compounds. Finally, we addressed the promise of geopolymers in future sectors, such as infrastructure repair, environmentally friendly systems, and applications in medicine, emphasizing their long-term viability and versatility in current materials science.

 Received 24th October 2024  
 Accepted 25th March 2025

 DOI: 10.1039/d4ra07601j  
[rsc.li/rsc-advances](http://rsc.li/rsc-advances)
<sup>a</sup>National Water and Energy Center, United Arab Emirates University, Al Ain, 15551, United Arab Emirates. E-mail: [rajwali@uaeu.ac.ae](mailto:rajwali@uaeu.ac.ae)
<sup>b</sup>Department of Physics, University of Wisconsin-La Crosse, WI 54601, USA. E-mail: [shahidiqbalphysics@gmail.com](mailto:shahidiqbalphysics@gmail.com)
<sup>c</sup>Department of Physics and Teaching Methods, Tashkent State Pedagogical University, Tashkent, Uzbekistan

<sup>d</sup>Department of Cybernetics, Nanotechnology and Data Processing, Faculty of Automatic Control, Electronics and Computer Science, Silesian University of Technology, Akademicka 16, 44-100 Gliwice, Poland

<sup>e</sup>Chemical Engineering Department, College of Engineering, University of Ha'il, P.O. Box 2440, Ha'il, 81441, Saudi Arabia

<sup>f</sup>Chemical Engineering Process Department, National School of Engineers Gabes, University of Gabes, Gabes 6029, Tunisia


Rajwali Khan

Dr Rajwali Khan is currently a researcher at the National Water and Energy Center, United Arab Emirates University, Al Ain, 15551, United Arab Emirates. His current research interests include design, fabrication, and exploring novel properties of organic and inorganic semiconductors and memristive devices, with a special focus on neuromorphic characteristics.



Shahid Iqbal

Dr Shahid Iqbal is currently an Assistant Professor of Physics at the University of Wisconsin-La Crosse. He received the PhD degree in experimental physics from Western Michigan University, Michigan, in December 2019. His current research involves the synthesis of metallic nanostructures, plasmonic, ion beam materials analysis, characterization of nanostructures, and the interaction between quantum emitters and nano-antennas.



## 1. Introduction

The synthesis, development, and application of geopolymeric materials have been extensively explored, primarily focusing on waste materials and indigenous or synthetic silico-aluminates. The composition and properties of geopolymer concrete made from soil and clay minerals have been fully analyzed. Geopolymers are man-made/inorganic polymers made from  $\text{Al}_2\text{SiO}_5$  minerals (which are composed of silicon, oxygen, and aluminum) and concentrated soluble base (alkali metals cations and hydroxide anions  $\text{OH}^-$ ) or a basic silicate media, *e.g.*,  $\text{Na}_2\text{SiO}_3$  or  $\text{Na}_2\text{O}_3\text{Si}$ . After that, a drying and curing process is performed at room temperature or a slightly warmer temperature in the range of 20–100 °C. According to Davidovits,<sup>1,2</sup> geopolymerization involves the reaction between an adequate quantity of responsive silicon dioxide ( $\text{SiO}_2$ ) and aluminum oxide ( $\text{Al}_2\text{O}_3$ ), resulting in the formation of geopolymers. Meanwhile, the solution should be an exceedingly strong basic solution. To put it another way, synthesis of a geopolymer involves strong fluid blends with powdered aluminosilicates, as shown in Fig. 1.

## 2. Geopolymer configuration along with nomenclature

The term/name “geopolymer” was coined by Davidovits.<sup>2,3</sup> The prefix “geo” signifies an inorganic aluminosilicate obtained from geological components that were polycondensed with an alkaline liquid to create a material.<sup>3</sup> As shown in Fig. 2(A)–(C), the recommended classification of geopolymer structures separates geopolymers into three essential types based on their silicon-to-aluminum proportions including  $\text{Si} : \text{Al} = 1$ ,  $\text{Si} : \text{Al} = 2$ , and  $\text{Si} : \text{Al} = 3$ .<sup>8–10</sup> Geopolymers are three-layered  $\text{Si}-\text{O}-\text{Al}$  polymeric organizations having an unpredictable to semi-glasslike structure.<sup>11,12</sup> All the oxygen particles are shared among the  $\text{SiO}_4$  and  $\text{AlO}_4$  tetrahedra, with Al in a precisely 4-fold connection, as shown in Fig. 3(a). The 4-fold coordinated Al carries as a negative charge, which is balanced by positively charged ions such as sodium, potassium, calcium, barium, ammonium, and hydronium ions. The presence of positively charged ions is essential to maintain the charge balance and structural stability of the material.<sup>13</sup> In any case, it is considered that as well as playing a charge-adjusting role, the positively

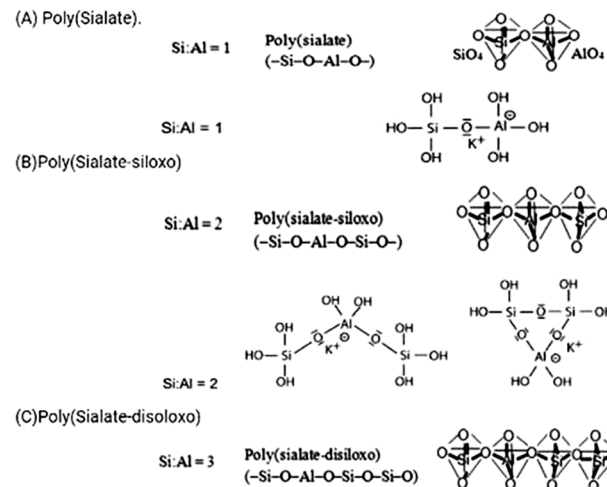


Fig. 2 (A)–(C) Various geopolymer systems based on the  $\text{Si} : \text{Al}$  ratio.<sup>8–10</sup>

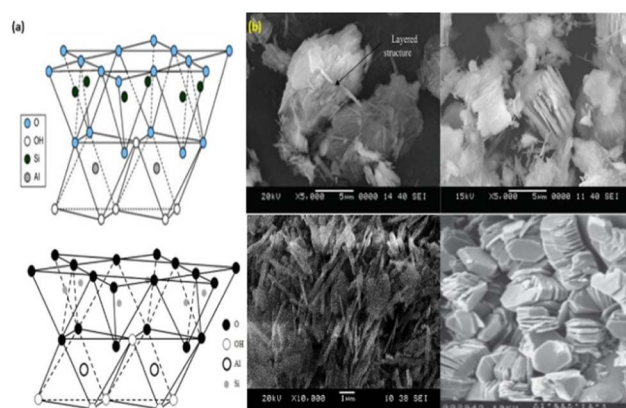
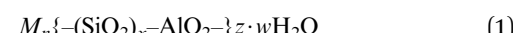


Fig. 3 (a) Kaolinite structure and (b) microstructure of kaolinite.<sup>4–7</sup>

charged particles are critical in deciding the eventual stability of the structure. As indicated by Saidi *et al.*,<sup>14</sup> the sodium (Na) cation impacts the stability of geopolymers. Geopolymers can be represented by the following general formula:



where  $M$  represents positively charged ions such as  $\text{Ca}^{2+}$ ,  $\text{Na}^+$  and  $\text{K}^+$ ;  $n$  represents the measure of polymer formation or degree of polycondensation;  $z$  represents 1, 2, 3..., and  $w$  represents the amount of water needed for binding.

## 3. Aluminosilicate sources

In the development of geopolymers, a variety of unrefined precursor substances have been utilized. Kaolinite was ordinarily utilized in the preparation of geopolymer composites in the early phases of development.<sup>10,15–17</sup> Other fundamental materials, such as calcined muds, were subsequently examined,<sup>18,19</sup> together with industrial waste such as ash,<sup>20,21</sup> rubbish

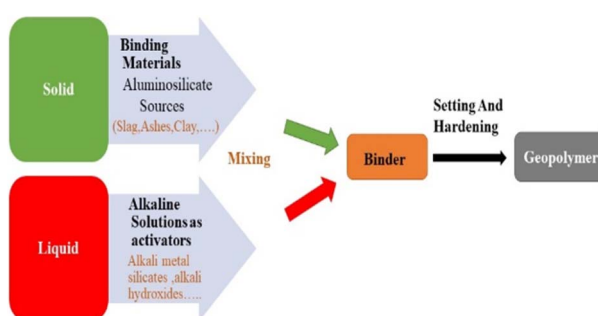


Fig. 1 Schematic of geopolymer formation.



glass,<sup>22</sup> and tailings from copper mines<sup>23</sup> also an assortment of extra regular and manufactured silicoaluminates (*e.g.* zeolite,<sup>24</sup>  $\text{Al}_2\text{O}_3\text{-}2\text{SiO}_2$ ) powder in its purest form,<sup>25</sup> and minerals containing magnesium.<sup>26</sup> Aluminosilicates, which are rich in alumina ( $\text{Al}_2\text{O}_3$ ) and silica, are the fundamental materials used to fabricate geopolymers ( $\text{SiO}_2$ ), which are abundant in the Earth's crust. These materials are significant sources of  $\text{Al}^{3+}$  and  $\text{Si}^{4+}$  particles in the framework, which assists in creating geopolymers, as shown in Fig. 3(A)–(C). The alumina and silica compounds in building materials should ideally be in a responsive shapeless state<sup>11,27</sup> with an overall proportion of over 70%. The usage of earth or dirt minerals in geopolymer development, as well as their design and attributes, are discussed in this work.

### 3.1 Composition of clay minerals

Kaolinite is a frequently used clay mineral in the synthesis of geopolymers. It is comprised of 1:1 uncharged dioctahedral layers with the formula of  $\text{Al}_2\text{O}_3\text{-}2\text{SiO}_2\text{-}2\text{H}_2\text{O}$  (Fig. 3(b)). These layers are comprised of two sheets,  $(\text{Si}_2\text{O}_5)_n$  and  $\text{Al}(\text{OH})_3$  (gibbsite), which are joined by oxygen molecules. As seen in Fig. 3(b),<sup>4–7</sup> van der Waals and hydrogen bonds<sup>28</sup> keep these sheets intact, delivering a sheet or layered design (SEM images). Gibbsite and  $\text{Si}_2\text{O}_5$  possess almost negligible electromagnetic charge and their sheets are arranged closely together, preventing substitution with other elements. Kaolinite possesses a small surface region for the polymerization process, in contrast to fly ash, which consists of spherical particles. Due to the small surface area of kaolinite, acid/alkali treatment is

limited, resulting in diminished strength.<sup>29</sup> Xu and van Deventer<sup>30</sup> used sixteen types of aluminum silicate ( $\text{Al}_2\text{O}_5\text{Si}$  or  $\text{Al}_2\text{SiO}_5$ ) materials as precursor materials for the formation of geopolymers (almandite ( $\text{Fe}_3\text{Al}_2\text{Si}_3\text{O}_12$ ),  $\text{Ca}_3\text{Al}_2\text{Si}_3\text{O}_12$ , fibrolite, cross stone, cyanite, hiddenite, pyroxene augite, lithia mica, hydromica, *etc.*). To achieve specific characteristics, some soil minerals require the incorporation of kaolinite as a strengthening agent. Regardless, utilizing kaolinite alone in the polymerization technique resulted in a frail design. Among them, stilbite had the most noteworthy compressive strength of 180 bars.

Furthermore, van Jaarsveld *et al.*<sup>31</sup> found that including a high concentration (41 wt%) of kaolinite in fly ash geopolymers affected the strength of the final product. This is due to the fact that not all the kaolinite participates in the geopolymerization, resulting in the formation of a geopolymer network. The compressive strength of kaolinite increases as it is calcined. Table 1 displays the compressive strength of calcined kaolinite, as determined by van Jaarsveld *et al.*<sup>31</sup>

### 3.2 Clay mineral pre-treatment

The pre-treatment of clay essentially affects the attributes of geopolymers. Geopolymers produced using heat-treated halloysite possessed average attributes, as reported by MacKenzie *et al.*<sup>32</sup> When mechanochemically treated halloysite was employed, an incomplete geopolymerization process was noticed. Table 2 presents the various types of clay minerals. Halloysite that had been synthetically treated in an acidic medium formed inadequately set geopolymers, while halloysite that had been treated with alkali for over 3 h resulted in the formation of crystalline zeolites that cured and hardened during the formation of geopolymers. The thermal treatment was performed at 200–1000 °C for 2 h during the examination. The materials were treated by soaking in either a basic (0.1 M sodium hydroxide) or acidic (0.1 M hydrochloric acid) solution for a period of 1 to 24 h, while mechanical and chemical curing were performed by high-energy grinding for 20 h at 400 rpm.

In general, geopolymers prepared *via* the thermal curing of raw materials such as metakaolin, fly ash, and impact heater slag have improved strength.<sup>30,40–42</sup> Heat treatment influences the reactivity of kaolinite in the geopolymerization process. When kaolinite is effectively calcined, it exists in an incredibly

**Table 1** Conditions for the calcination of metakaolinite, and their effects on the compressive strength of fly-ash based geopolymers with additional variables: metakaolinite (clay) content = 14 wt%, water to fly ash mass ratio = 0.31,  $\text{K}_2\text{O}/\text{SiO}_2$  = 1.14, and alumina to silica ratio = 0.57 (ref. 31)

Time (h)	Temperature (°C)						
	300	400	500	600	700	800	900
1	14	14	30	54	17	7	8
6	11	31	13	9	15	7	15
12	12	47	28	25	14	3	15
24	6	32	31	18	6	15	12

**Table 2** Different types of clay minerals

Clay mineral	$\text{SiO}_2$	$\text{Al}_2\text{O}_3$	$\text{CaO}$	$\text{K}_2\text{O}$	$\text{Na}_2\text{O}$	$\text{Fe}_2\text{O}_3$	$\text{TiO}_2$	$\text{MgO}$	$\text{P}_2\text{O}_5$	LOI	$\text{SO}_3$	$\text{MnO}$	References
Metakaolin	51.35	44.24	0.13	0.08	0.16	0.98	0.90	0.48	0.45	0.72	—	0.01	33
Metakaolin	52.1	43.0		2.5	0.12	0.7	—	0.3	—	1.0	—	—	34
Metakaolin	59.7	34.1	0.1		0.2	0.9	—	—	—	1.2	0.12	—	35
Occhito lake clay, Italy	47.5	15.6	10.2	1.9	0.3	6.7	—	2.4	—	15.4	—	—	36
Sabetta port clay, Italy	50.0	15.9	6.9	1.7	0.3	5.7	—	1.9	—	17.5	—	—	37
Kaolinite from Jordan	48.92	25.16	0.68	1.4	0.21	7.52	0.86	0.21	0.16	11.93	2.94	0.01	38
Kaolinite	49.35	36.03	0.02	2.29	0.04	0.20	0.02	0.02	—	11.94	—	—	39
Kaolinite	40.86	39.87	0.12	0.17	0.01	0.39	0.46	0.12	—	17.91	—	—	39
Kaolinite	42.66	40.92	0.14	0.09	0.14	1.12	0.45	0.04	—	14.13	—	—	39
Halloysite	48.12	36.33	0.04	0.03	0.04	0.33	0.16	—	—	14.8	—	—	39



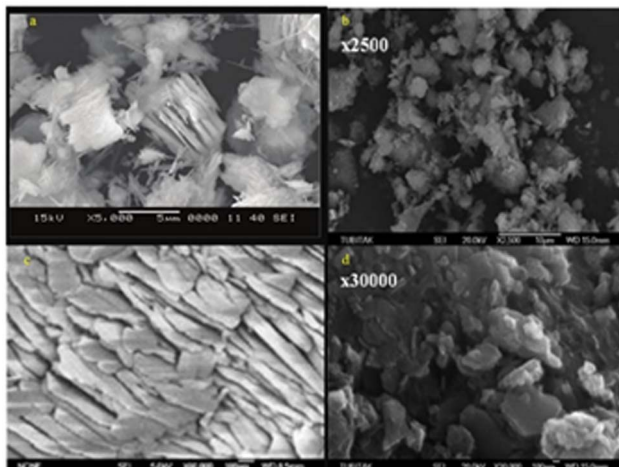


Fig. 4 (a)–(d) SEM micrographs of metakaolin calcined at different temperatures.<sup>6,43,44</sup>

pozzolanic formless state, as shown in Fig. 4(a)–(d). Thermal curing converts the translucent state to responsive indistinct states.<sup>45</sup> These shapeless states undoubtedly give dynamic constituents that characterize the final strength of the geopolymer. At 550–800 °C, the fixed fortified hydroxyl particles on the aluminium built-in sheet dehydroxylate due to H<sub>2</sub>O dehydration during the thermal treatment of kaolinite.<sup>46</sup> This transforms kaolinite into the disordered metastable stage of metakaolin. Despite undergoing treatment method, metakaolin maintains its layered structure. This is because the layered structure of metakaolin seems to be more open than that of kaolinite.<sup>47,48</sup>

Besides, atomic changes and rearrangement of the hexa-coordinated Al particles in kaolinite into penta- and tetra-coordinated Al particles destroys its hexagonal layer.<sup>49</sup> In this case, the amount of hexa-coordinated Al particles converted to penta- and tetra-coordinated Al particles determine the reactivity of metakaolin. When the content of hexa-coordinated Al particle is the lowest, metakaolin has the greatest reactivity.<sup>48</sup> The thermal curing range of kaolinite is typically between 599 °C and 899 °C. Rowles and coworkers<sup>50</sup> showed that receptive metakaolin can be prepared by warming kaolinite at 749.5 °C in air for 24 h. The MAS NMR examination uncovered an exceptionally cluttered organization of metakaolin with wide vibrations of ~104.8 ppm and Q<sup>4</sup> of ~111.5 ppm. Singh *et al.*<sup>51</sup> employed the same calcination temperature, but for a brief duration of 10 h. Alternatively, Guo *et al.*<sup>36</sup> found that the optimized conditions were calcining kaolin at 800 °C for 2. Metakaolin was employed to produce low-strength geopolymers when heated at more than 900 °C. Overall, this can be attributed to calcination, which resulted in a difference in responsive nebulous stages into dead consumed and non-receptive mullite crystalline phases. Then, the ideal calcination at 900 °C was recorded. Zhang *et al.*<sup>28</sup> recorded the XRD diffractogram of their geopolymer, which displayed that the activity of the annealed materials improved with an increase in temperature in the dehydroxylation area but dropped sharply in the “spinel” zone.

The translucent pinnacles of kaolinite became more fragile as the temperature increased. This suggests that the crystalline structure of kaolin was destroyed. Alternatively, a calcination temperature of kaolin in the range of 649–849 °C had no significant impact on the mechanical properties of the geopolymers, as reported by Kong *et al.*<sup>52</sup> As the Si/Al proportion increased from 1.40 to 1.54, the impact of calcination temperature became more obvious. With an Si/Al proportion of 1.54, the most elevated strength of 45 MPa was achieved at a calcination temperature of 750 °C. The surface area of the unrefined components was expanded upon heat treatment. Ferone *et al.*<sup>53</sup> observed that calcining supply mud/clay silt/sediment at 400 °C and 750 °C for 2 h before alkalination increased the disintegration of the clay sediments. The compressive strength of the clay samples treated at 750 °C was higher (between 6 and 12 MPa) than that cured at 400 °C (between 1 and 4 MPa). It was shown that the treated unrefined components had an enormous surface region for alkali/basic reactant disintegration, ensuing a geopolymer process response.

Calcination has been reported to be performed in the air using heater. Kolousek *et al.*<sup>54</sup> utilized an alternative calcination strategy. In their study, an inferior class of kaolin was used for calcination with a blend of sodium hydroxide and potassium hydroxide. After calcination, the substance was ground and blended directly with H<sub>2</sub>O(l) (instead of a salt reactant) for the production of a geopolymer. This geopolymer was named a one-part geopolymer. However, the final product had a strength of 1 MPa. Feng *et al.*<sup>55</sup> created geopolymers with adequate compressive strength of 40 MPa after treatment for 4 weeks, compared to that reported by Kolousek *et al.*<sup>54</sup> The final sample was obtained *via* the calcination of albite with soda ash (Na<sub>2</sub>CO<sub>3</sub>) or caustic soda (NaOH). Ke and co-researchers,<sup>56</sup> Peng and co-workers,<sup>57</sup> and Nematollahi and co-researchers<sup>58</sup> performed comparative studies; however, they used different unrefined components such as bauxite residue, coal ash, slag, and calcium hydroxide. The interest in this field of examination is critical given that it can possibly expand the application and cost-effectiveness of geopolymers.

### 3.3 Geopolymers made of clay (clay-based geopolymers)

Commonly, clay is utilized as the starting material for geopolymers given that it accommodates straightforward translation of the outcomes and disposes of the requirement for modern understanding. Due to the presence of debasements and impurities, the use of unrefined components, for example, fly ash and slag, may affect the outcome. Clay is rich in Al<sub>2</sub>O<sub>3</sub> and SiO<sub>2</sub>, with an overall content of 70–90% of both. Generally, the structure of clay varies depending on its source and geographical location. The impact of changing variables such as silicon to aluminium and sodium to aluminium molar proportions, explicit surface and synthesis of dirt, soluble base centralization of alkali reactant arrangement, modulus of alkali silicate arrangement, treatment conditions, *etc.* has been widely investigated in metakaolin geopolymers to date.<sup>38,59,60</sup> Metakaolin geopolymers are not compact. The layer structure



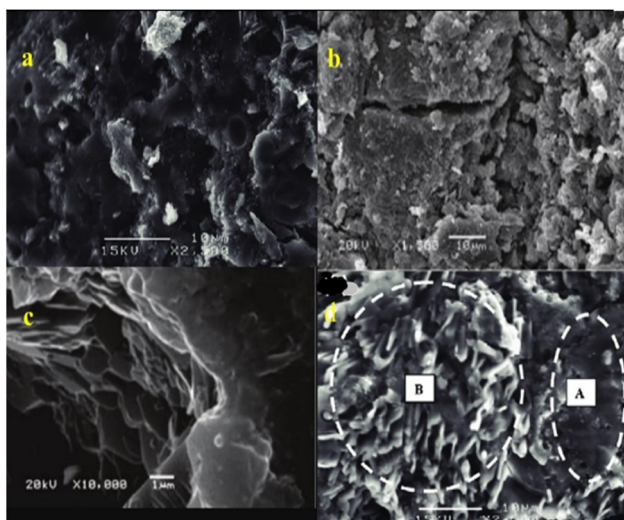


Fig. 5 SEM images of (a)–(c) pure metakaolin and (d) metakaolin geopolymer with slag where ("A" shows geopolymer matrix and "B" shows CSH gel).<sup>6</sup>

remains in the geopolymer matrix after the geopolymerization reaction,<sup>6</sup> as shown in Fig. 5(a)–(d).

A few analysts prepared blended geopolymers as opposed to utilizing metakaolin alone in geopolymer amalgamation. Metakaolin is combined with other initial reactants such as  $\text{Ca}(\text{OH})_2$ , ash, and cinders. In the geopolymer network, these unrefined components act as both a fastener/binder and a filler. Alonso *et al.*,<sup>61,62</sup> for instance, combined  $\text{Ca}(\text{OH})_2$  with metakaolin and discovered that  $\text{Ca}(\text{OH})_2$  had no effect on the final results. Moreover, Yunsheng *et al.*<sup>63</sup> showed that adding 30% slag to metakaolin geopolymers further enhanced their strength. However, if more than 50% slag was applied, the strength was reduced. The mechanical characteristics of the final result were upgraded by filling huge grains of slag.<sup>49</sup>  $\text{CaH}_2\text{O}_4\text{Si}$  (C-S-H) phase was created in the blend with the geopolymer matrix considering the fact that both  $\text{Ca}(\text{OH})_2$  as well as slag have a high "Ca" concentration. Yunsheng *et al.*<sup>63</sup> made microstructure geopolymers, given that the unadulterated metakaolin geopolymer only displayed one homogenous phase, though the slag-metakaolin geopolymer had two obvious phases (CSH and geopolymer framework). Buchwald *et al.*<sup>64</sup> reported similar observations.

#### 4. Alkali reactant

A solvent alkali metal, namely, sodium or potassium, is utilized as a salt reactant. Alkali silicates, hydroxides, carbonates, and additives such as sodium aluminates and concrete oven dust are used. Aluminosilicates quickly disintegrate in solid basic media, delivering silicon–oxygen tetrahedral and  $\text{AlO}_4$  tetrahedral units and enhancing the disintegrated species for polycondensation.<sup>65,66</sup> A solution of hydroxides (sodium hydroxide and potassium hydroxide) and silicates is the most well-known alkali reactant solution (sodium silicate and potassium silicate).<sup>16,45,67</sup>

#### 4.1 Sodium or potassium-based alkaline solution

Alkalinity is accomplished utilizing  $\text{NaOH}$  or  $\text{KOH}$  solutions. The limit of different aluminosilicate sources to filter  $\text{NaOH}$  and  $\text{KOH}$  has been widely observed. The disintegration of aluminosilicate sources regularly increases as the concentration of alkali solution increases. The limit of a geopolymer to disintegrate is often related to its final strength.<sup>30</sup> However, a large number of researchers concluded that  $\text{Al}_2\text{SiO}_5$  materials dissolve better in sodium hydroxide than in potassium hydroxide. The geopolymers created using  $\text{Al}_2\text{SiO}_5$  material had higher compressive strength in potassium hydroxide than in sodium hydroxide solution, despite its higher dissolution in  $\text{NaOH}$  solution, as shown in Fig. 6. Panagiotopoulou *et al.*<sup>68</sup> explored the limit of  $\text{Al}_2\text{SiO}_5$  to leach in 10 M sodium hydroxide and potassium hydroxide solutions, individually, as shown in Fig. 6. The aluminosilicates broke down more promptly in  $\text{NaOH}$  than in  $\text{KOH}$ , forms expected.

The ability to leach was found to decrease in the order of kaolin > metakaolin > zeolite > slag > fly debris > pozzolana, as shown in Fig. 7(a). More  $\text{Na}^+$  particles were easier to combine with the silicate anion to form smaller oligomers, according to Xu and van Deventer.<sup>30</sup> Overall, when more  $\text{K}^+$  particles combined with the silicate anion, larger oligomers were formed. Therefore, the compressive strength of the K-based geopolymers was 42% greater than that of the Na-based geopolymers. In the case of kaolinitic material, a comparable example was seen.<sup>27</sup> Also, greater  $\text{K}^+$  particles help in the setting of geopolymers.<sup>72</sup> Steveson and Sagoe-Crentsil<sup>71</sup> detailed a captivating outcome. The microstructure of geopolymers made with K and Na alkali solution is displayed in Fig. 7(a)–(d). The geopolymer had a more obvious geopolymer grid, as shown by globular units and less unreacted metakaolin particles in its

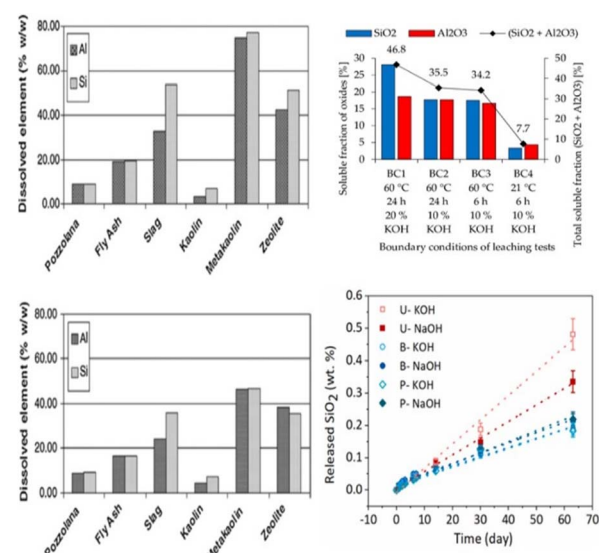


Fig. 6 Aluminium (Al) and silicon (Si) were dissolved in 10% 10 M  $\text{NaOH}$  and  $\text{KOH}$  solutions, respectively. The soluble fraction of oxides and the total soluble fraction of oxides of metakaolin were analyzed. Additionally, the release of  $\text{SiO}_2$  from different aggregates in 0.4 M  $\text{NaOH}$  and  $\text{KOH}$  solutions was measured as a function of time at 38 °C.<sup>68–70</sup>

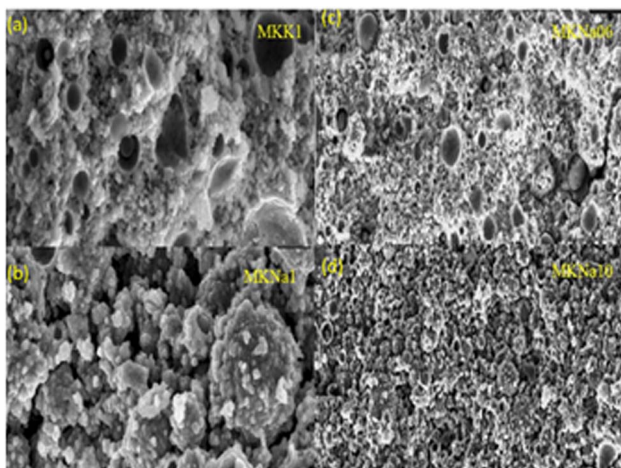


Fig. 7 Metakaolin geopolymers of the same composition made with different activating cations (MKK1 shows geopolymers prepared with (a) K-based activating alkali solution, while (b) MKNa1 shows geopolymers prepared with Na-based alkali solution, while (c) MKNa06 and (d) MKNa10 show different molarity of sodium alkali solution).<sup>71</sup>

morphology (layered design). In this case, the K-based geopolymers possessed a better surface and a denser design. The Na-based geopolymers had a better compressive strength than the other geopolymers, as observed in their SEM images. The smaller  $\text{Na}^+$  particles are believed to be more dynamic in soluble base responses, bringing about superior disintegration and adjustment of the silicate monomers and dimmers. Rahier *et al.*<sup>73</sup> performed a DSC investigation to confirm this outcome. Lizcano *et al.*<sup>74</sup> reported comparable examples of microstructures. In any case, the compressive strength estimation varied from that reported by Steveson and Sagoe-Crentsil.<sup>71</sup> Despite the fact that the Na-based soluble base reactant is thicker and responds faster, it prevents the creation of a homogenous design, resulting in a permeable structure and lower strength. Regardless, the Na-based alkali reactant is preferred for geo-polymer alkalination given that this method is more practical.

#### 4.2 Mixture of alkali silicate solution and alkali hydroxide

Although alkali hydroxide is fundamental for aluminosilicate disintegration, soluble base silicate can act as a fastener, alkali reactant, dispersant, and plasticizer.<sup>75</sup> Besides  $\text{Na}_2\text{SiO}_3/\text{K}_2\text{SiO}_3$  solution, silica seethe/fume can be utilized as another option or additive to metal silicate. Currently, they are used to examine of geopolymers created with soluble base hydroxide *versus* a mixture of basic hydroxide and metal silicate arrangements, as shown in Fig. 8(a)–(d). The presence of alkali silicate in the alkali reactant combination is vital according to most examinations, resulting in an microstructure and strength characteristics. Also, it affects the particular extent of solvent  $\text{SiO}_2$  structures, including monomers, dimmers, and oligomers, in the alkali silicate arrangement/solution.<sup>51</sup>

A change in the silica content of the combination<sup>13</sup> resulted in improve silicate gelation and precipitation. NaOH-activated kaolin geopolymers had a compressive strength of 20 MPa, as

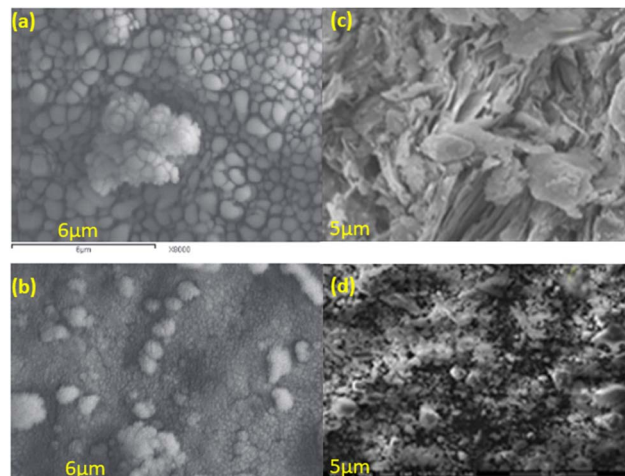


Fig. 8 SEM images of (a) and (b) kaolin made with NaOH solution and (c) and (d) kaolin made with alkaline sodium silicate solution.<sup>76,77</sup>

reported by Mohsen and Mostafa<sup>77</sup> (Fig. 8(c) and (d)), while soluble sodium silicate-activated kaolin geopolymers had a compressive strength of 60 MPa. Pacheco-Torgal *et al.*<sup>40</sup> found a comparative strength design. The kaolin geopolymers made with  $\text{Na}_2\text{SiO}_3$  arrangement possessed a fine texture and a high-density construction, as seen in their microstructure images. This suggests an enhancement in the sodium silicate geo-polymerization response.

Ferone *et al.*<sup>53</sup> reported comparable results, as shown Fig. 9(a)–(d). Although the compressive strength of the NaOH-activated and  $\text{NaOH}-\text{Na}_2\text{SiO}_3$ -activated geopolymers was comparable, their microstructures were significantly different. The minimal construction created when responded with the  $\text{NaOH}-\text{Na}_2\text{SiO}_3$  mixture showed the more viable alkalinization of Al and Si. Because of its dissolvable silicate content, which will,

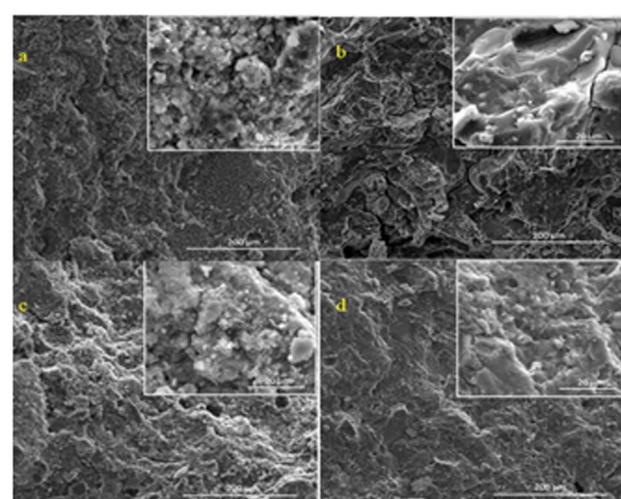


Fig. 9 SEM micrographs of geopolymers made using (a) NaOH solution and (b) combination of NaOH and  $\text{Na}_2\text{SiO}_3$ /sodium silicate solutions using clay particles from the Occhito reservoir. (c) and (d) Blast furnace slag was used as a supplement/additive after the clay sediments were subjected to heat at 750 °C.<sup>53</sup>



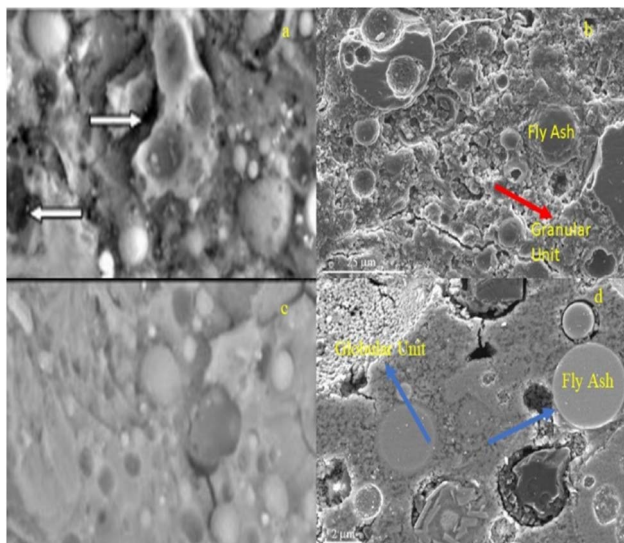


Fig. 10 SEM images of fly-ash-based geopolymers made with (a)–(c) NaOH solution and (d) alkaline silicate solution.<sup>78–80</sup>

in general, modify the speed of the geopolymerization activation, fluid metal silicate is inclined toward antacid/alkali silicate arrangement/solution in the formation of geopolymers.<sup>73</sup>

Moreover, alkalination of  $\text{Al}_2\text{SiO}_5$  with strong antacid/alkali without solution of alkali silicates yields products that fluctuate from geopolymers, as indicated by Davidovits.<sup>81</sup> A translucent zeolite or hydroxysodalite as opposed to fly debris geopolymers was obtained when the antacid/alkali silicate-activated fly debris/ash geopolymer framework had globular units as geopolymerization proceeded. Translucent/crystalline and granular designs were found in the NaOH-activated fly debris geopolymer, as shown in Fig. 10(a)–(d).<sup>78–80</sup> In addition, geopolymers were formed using a mixture of alkali reactant solutions of potassium silicate/sodium hydroxide, sodium silicate/sodium hydroxide, and potassium silicate/potassium hydroxide. Alkali reactant solutions of the same alkali elements (sodium silicate/sodium hydroxide and potassium silicate/potassium hydroxide) usually outperform different alkali metal reactant solutions in terms of strength. This was attributed to the fact that potassium silicate has a quicker polycondensation rate than sodium silicate, resulting in more salt elements participating in the polycondensation interaction instead of aluminosilicate disintegration.<sup>72</sup> Geopolymers containing sodium silicate set faster than that containing potassium silicate, according to Kong *et al.*<sup>52</sup> O'Connor and Mackenzie<sup>82</sup> utilized a lithium-based salt reactant to make halloysite geopolymers besides Na and K-based antacid/alkali reactants. Because of the reactant impact on gel development and stage division, the final results did not properly show the common nebulous element/final product of geopolymers, but instead lithium zeolites.  $\text{Na}_2\text{CO}_3$ ,  $\text{K}_2\text{CO}_3$ , and  $\text{K}_2\text{SO}_4$  may be utilized as salt reactants, in addition to the previously mentioned normal alkali reactant solutions.<sup>13,83,84</sup> Clay-based geopolymers definitely stand out to be noticed with the above-mentioned alkali reactants.

## 5. Reactions occurring during the formation of geopolymers (geopolymerization process)

The reactions happening during the geopolymer formation process are synthetic reactions, in which aluminosilicate ( $\text{Al}_2\text{SiO}_5$ ) materials change to some extent or completely from an amorphous phase into 3D polymer organizations rapidly. The alkali reactant and the type of ( $\text{Al}_2\text{SiO}_5$ ) material used decide the science of alkalination. The geopolymer combination employing a comparable system for understanding the response that prompts the formation of geopolymers is vital. The particular geopolymerization response was only recently revealed.<sup>85</sup> Most investigations concur that the formation of geopolymers involves dissolving Al and Si species from aluminosilicate surfaces, cross-linking (polymer formation process) of dynamic plane assemblies and solvent atoms and ions forming a gel, which afterward solidifies to shape an unbending strong material known as a geopolymer.

### 5.1 Reaction occurring during the formation of geopolymers (geopolymerization process)

As mentioned, kaolinite-based geopolymers have an overlay construction, as well as ionic charges, which prevent ion interchange after interaction with soluble base reactants. As a result, the kaolinite layer chemical attack begins at the outward area and borders, and gradually perforates the structure layer by layer, as shown in Fig. 11.<sup>6</sup> This becomes the primary reason for the poor strength performance of almost all geopolymers made using clay or soil. Meanwhile, the production of aluminium-substituted silicate layers after attack by sodium hydroxide solution is depicted in a schematic model in Fig. 12.<sup>6,86</sup> Structure-damaged aluminum sites were produced and changed into tetra-organized aluminum sites after the chemical attack.

### 5.2 Reaction mechanism

Geopolymerization is a heat-releasing reaction that is thought to be carried out by oligomers (dimers and trimers) that supply

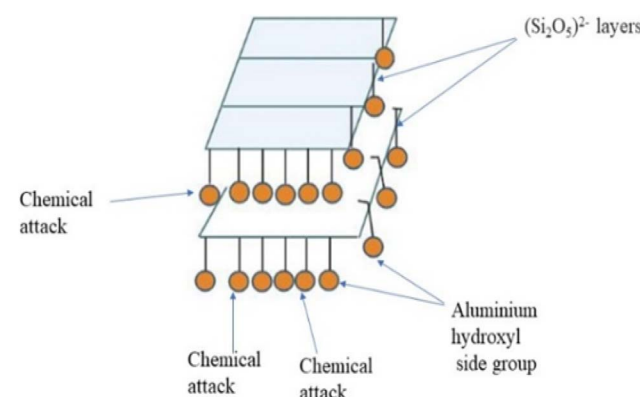


Fig. 11 Chemical attack on kaolinite layers (orange circles represent aluminium hydroxyl side group).<sup>6</sup>



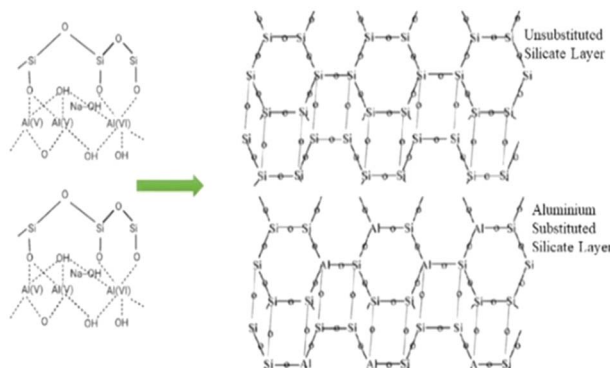


Fig. 12 Schematic showing the unsubstituted silicate layer and substituted aluminium silicate layer after interaction of metakaolin with NaOH solution.<sup>6,86</sup>

the real unit structures of three-dimensional macromolecular structures. The equations for geopolymers production proposed by Kong,<sup>52</sup> Davidovits and Heah<sup>1,87</sup> are shown in Fig. 13, where  $(\text{Si}_2\text{O}_5, \text{Al}_2\text{O}_2)$  refers to the IV-fold coordination of Al, while  $\text{SiO}_2$  comes from a silicate solution. The backbone of the final product is Si–O–Al. The existence of  $\text{OH}^-$  in the soluble base reactant starts the breakdown of  $\text{Al}_2\text{SiO}_5$  in alkaline media, releasing  $(\text{Si}_2\text{O}_5^{2-})_n$  and  $(\text{AlO}_3^{1-})$  ions to aid in the geopolymers formation process.<sup>75</sup> The amount of disintegration is determined by fine grains, the capability of ion interchange, the alkaline solution concentration, and the structure of the precursor materials. The polymerization reaction is thought to take place in many steps that occur at the same time,<sup>31,62,88</sup> as follows:

- Aluminosilicates disintegrate in an unequivocally alkaline reactant;
- Strong state changes and solidifying/hardening to create hard strong/solid;
- Depolymerization to create  $\text{Al}_2\text{SiO}_5$  gel phases; and
- Strong state change and solidifying to frame a strong geopolymers.

Also, Xu and van Deventer<sup>89</sup> introduced a response system for the union of geopolymers, as displayed in eqn (2)–(4). The creation of geopolymers occurs in eqn (4). The time expected for the Si–Al material to be consumed is not determined by the unrefined substance handling conditions.<sup>75</sup>

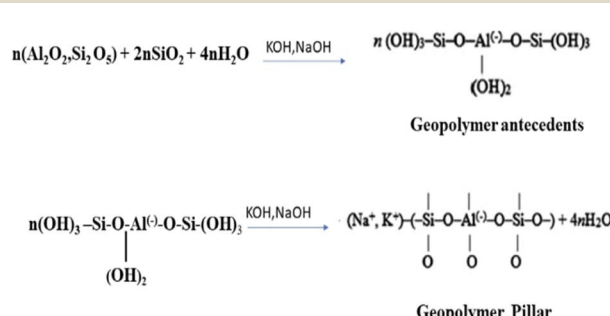
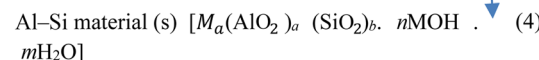
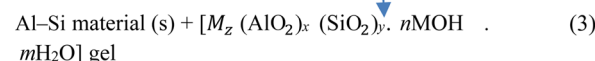
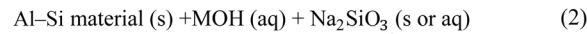


Fig. 13 Diagram showing polymerization process.<sup>1,87</sup>



The underlying geopolymers gel phase is distinct from a definitive gel phase after broadened restoration, as indicated by researchers<sup>90,91</sup> and shown in Fig. 14. During restoration, the gel phase goes through a steady adjustment toward more prominent crosslinking, with unbound water being released and the creation of some zeolitic crystallites. In their model, the beginning and last gel phases are addressed by the “hardening and solidifying” and “ongoing gel reworking and crystallization”, separately. More arranged phases are shaped in the end product.

When Si–O–Si and Si–O–Al covalent bonds contact an alkaline solution during geopolymers formation, they dissociate into a colloidal phase. Most researchers accept that the disintegrated items associate/interact and produce a coagulated design.<sup>92</sup> As the activation continues, the intermediate (Gel 1), having a high content of aluminium, is reorganized into Gel 2, which contains a higher content of Si, as shown in Fig. 15. Finally, the gel creates and delivers three-layered designs. The paradigm followed was very similar to that reported by Provis *et al.*,<sup>93</sup> in which the reaction involved the continuous arrangement of the gel into three-dimensional geopolymers structures.

Geopolymers structures are formed at an incredibly fast rate. The previously mentioned process is considered to happen at the same time. Also, the activation energy and reaction kinetics

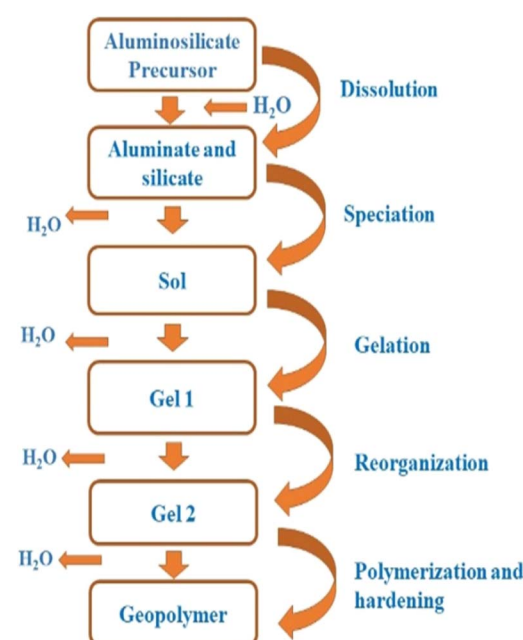


Fig. 14 Processes occurring during geopolymers formation.<sup>90,91</sup>



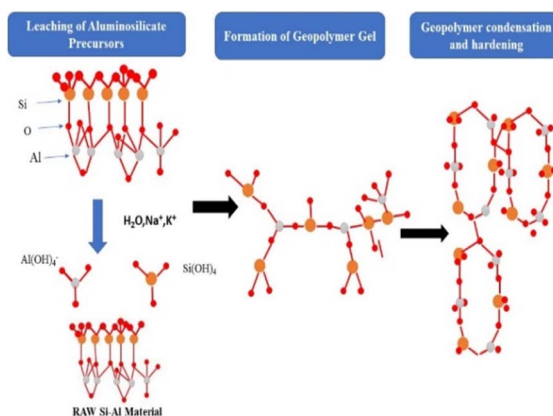


Fig. 15 Graphical model of geopolymerization process (orange circle represents Si, red circles represent "O" and grey circles represents "Al").<sup>92</sup>

are interconnected.<sup>94</sup> Thus, it is difficult to isolate the activation steps in tests.

### 5.3 Geopolymer formation

A homogenous geopolymer mixture with remarkable strength is the final result of the optimal mixture. The best known technique for producing geopolymers is the direct mixing of aluminosilicates with a soluble base reactant. After projecting and embellishing, the geopolymer glue is reconstituted at room temperature or at a slightly higher temperature. A thin coating of plastic is applied to the exposed surface to prevent damage from excessive moisture or dampness. Various mixing successions have also been used. To create kaolin/white soil slag mixed geopolymers, one method involves the use of the previously mentioned conventional blending procedure. In the next step, the aluminosilicates are combined with fluid or liquid sodium silicate, and after 3 min, an NaOH solution or solution is applied.<sup>49</sup> Neither approach was successful in reducing the level of geopolymerization. However, the last approach was detrimental to the mechanical strength given that the mixture contained too much water. Rattanasak and Chindaprasirt<sup>95</sup> uncovered incongruous discoveries in the example of fly debris geopolymers. Given that more time is allowed for the filtering of aluminosilicates, which affects the reaction, the subsequent procedure produced stronger geopolymers in comparison to the main technology. The type of underlying materials used and the ratios of blending and mixing determine whether a modified blending arrangement may enhance the geopolymerization process. To achieve a good consistency, an excessive amount of water is anticipated during the blending process in the clay testing. Compared to fly ash-based blends or mixtures, clay-based mixtures are usually gooier and tackier.<sup>96</sup> This is due to the layer-like structure of dirt, which reduces their usefulness for everyday tasks. Alternatively, fly ash is comprised circular particles, which reduce the inter-particle friction or between-molecule erosion, while also making the geopolymer mixture more usable. This can explain the superior mechanical properties of fly ash-based geopolymers. Functionality is an

important factor to consider in the design of geopolymers. Compaction will become problematic and result in a permeable/porous and sensitive final design if there is a real functioning problem.

## 6. Structural characterization of clay-based geopolymers

### 6.1 Morphology of clay-based geopolymers

Microstructural investigation can be performed to follow the development of geopolymers with time. The thickness and porosity of a geopolymer structure are firmly associated with its solidity. Low porosity, high thickness, and fine-grained microstructures are factors that contribute to the formation of high-strength geopolymers overall,<sup>71</sup> as shown in Fig. 16.

The SEM pictures recorded by different researchers<sup>97-99</sup> are displayed in Fig. 17(a)-(d). The layered design of metakaolin geopolymers was protected during the geopolymerization process. This upholds and confirms the guarantee by Davidovits<sup>81</sup> that the response happens on the outer layer of geopolymers.

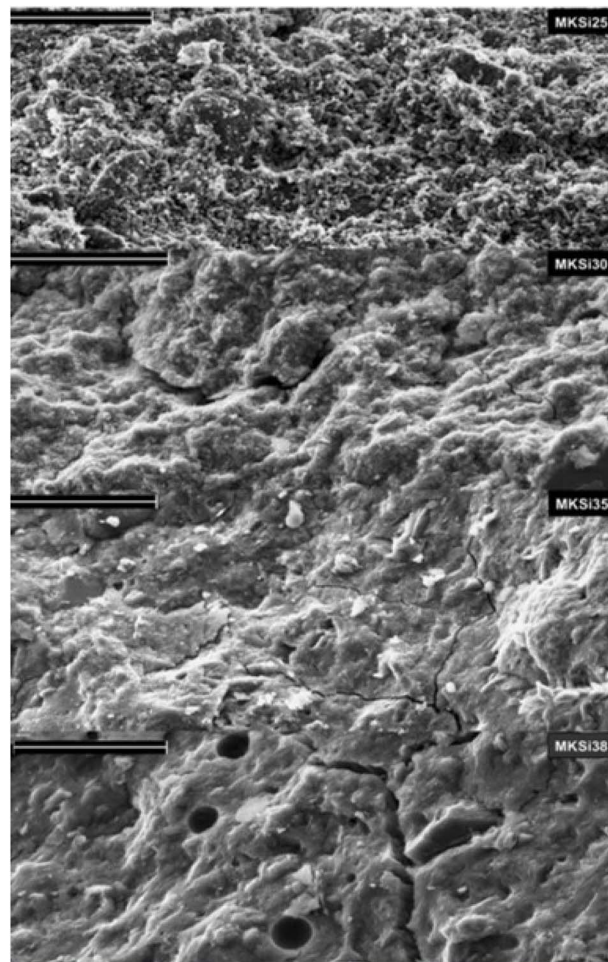


Fig. 16 SEM images show low porosity, high thickness, and fine-grained microstructures are factors that contribute to the formation of high-strength geopolymers.<sup>71</sup>



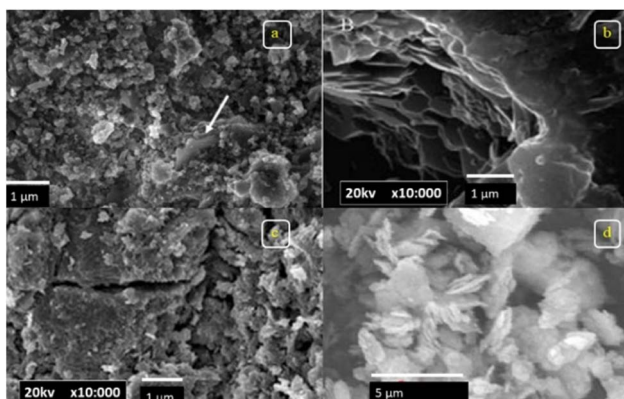


Fig. 17 (a)–(d) SEM images obtained for metakaolin geopolymers.<sup>97–99</sup>

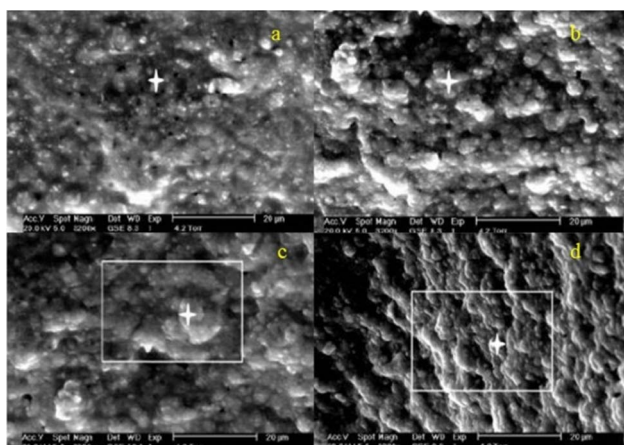


Fig. 18 ESEM micrographs obtained for the same area at different mixing times of (a) 10 min, (b) 3 h, (c) 6 h and (d) 9 h.<sup>86,100,103</sup>

The precipitation of film-like geopolymer globular units on the outer layer of approximately spaced metakaolin particles, along with densification and continuous formation of a dense geopolymer network within and around the voids, was observed in the microstructure of metakaolin geopolymers processed for an extended period, as displayed in Fig. 18(a)–(d).<sup>86,100,103</sup>

The existence of residual particles in the bulk geopolymer structures, according to Rowles *et al.*,<sup>50</sup> constitutes a stress concentration site, which generates cracks and fractures. Furthermore, leftover particles may modify the nominal composition of the geopolymer, preventing the complete growth of the geopolymer network.

Fly ash geopolymers are different from metakaolin geopolymers in that they are heterogeneous materials, for example, the non-responsive fly ash particles left in the empty spaces to some extent dissolve fly ash particles, as shown in Fig. 19(a)–(d). Non-responsive particles serve as filling particles and help to reinforce the composite. Instead of globular units in the geopolymer matrix in metakaolin geopolymers, a smooth and connected geopolymer matrix was discovered in fly ash-based geopolymers.

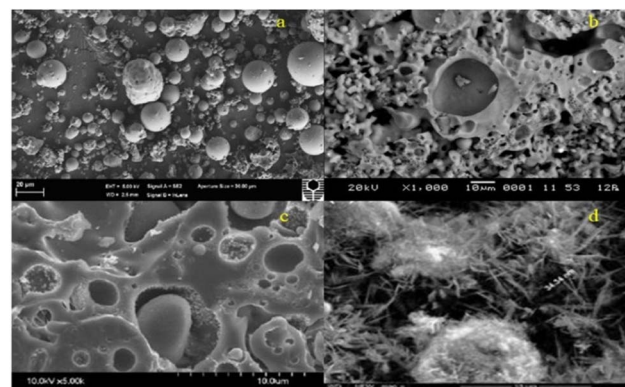


Fig. 19 SEM micrographs of (a) fly ash-based geopolymer, (b) fly ash-based geopolymer after calcination at 400 °C, 600 °C and 800 °C, (c) fly ash-based geopolymer calcined and cured at room temperature for 24 h and at 80 °C for another 24 h and (d) fly ash-based geopolymer prepared at 80 °C.<sup>18,101,102</sup>

## 6.2 Geopolymer phases

As per X-ray diffraction (XRD), geopolymers are completely amorphous. As outlined in Fig. 20 (left side panel and a–d), they frequently have a diffuse hollow peak in the  $2\theta$  range of 27–30°.<sup>104,105</sup> In accordance with the broad diffuse hump, the shapeless aluminosilicates, which contain a substantial cover, purposefully relax the geopolymer structure and increase its strength. The slope of this diffuse halo is determined by the Si/Al ratio. As the Si/Al proportion increases, the hump level decreases.<sup>74</sup> Similarly, Wang *et al.*<sup>97</sup> found response items with halo diffuse qualities somewhere in the  $2\theta$  range of 18° to 25° for metakaolin geopolymers. The quartz phase was demonstrated to be inert after alkalination. In any case, because of inadequate calcination, the impurities in kaolin decline in intensity.<sup>38,106,107</sup> Related to the indistinct phase of geopolymers, the development of crystalline phases, eminently zeolites, can be identified in the X-ray diffraction pattern of geopolymers, as shown in Fig. 21(a)–(c).<sup>81,108,109</sup> Geopolymers are substances that are equivalent to zeolitic materials. Geopolymers are in some cases considered to be a zeolitic precursor. Geopolymers and zeolites differ in that geopolymers are shapeless, while zeolites are translucent in nature.<sup>13,17,49</sup> Crystals inside geopolymers are managed by the curing temperatures, as well as the curing time

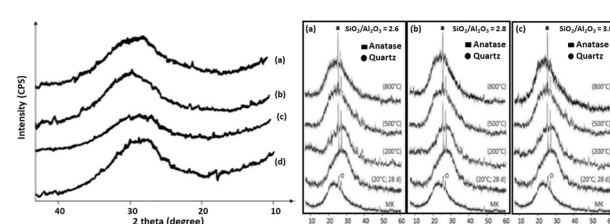


Fig. 20 (Left side panel) XRD diffractograms for poly(silicate-siloxo) geopolymers with molar ratios of  $\text{SiO}_2/\text{Al}_2\text{O}_3$  of (a) 4.02; (b) 3.98; (c) 3.39; and (d) 4.11. (Right) (a)–(c) XRD diffractograms of geopolymers with different  $\text{SiO}_2/\text{Al}_2\text{O}_3$  ratios and cured at different temperatures.<sup>104,105</sup>

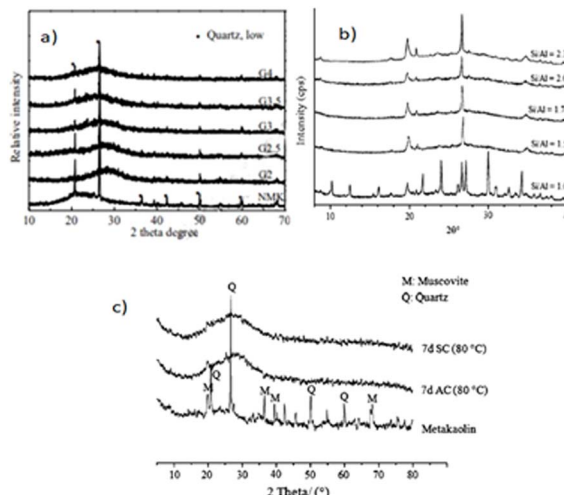


Fig. 21 XRD patterns of (a) geopolymers with different Si/Al ratios (NMK = metakaolin, G = Si/Al ratio) and (b) metakaolin made with alkaline sodium silicate solution with different Si/Al ratios and cured at 50 °C for 24 h.<sup>108,109</sup> (c) XRD patterns of geopolymers at calcining/curing temperature of 80 °C for 28 days (A = amorphous phase = quartz) (AC = air curing, SC = steam curing).<sup>38,81,106–109</sup>

and the type of alkali used. The crystallization of zeolites is supported by a high water content, a high calcination temperature, and a long curing length/time.<sup>12</sup> The quantity of zeolite crystallites increases with aging.<sup>110</sup> Zeolites are known for their permeable nature and poor mechanical qualities. It was once imagined that the amount of crystalline phase that the lattice could support was restricted 100% of the time. A few researchers<sup>54,111</sup> noticed that zeolite crystals strengthen the geopolymer matrix and increase its toughness; however, its overall strength is altogether diminished. Fly ash geopolymers have shown a comparable strength development design.<sup>112</sup>

### 6.3 Identification of functional groups

FTIR spectroscopy can be utilized to offer data on the progress of vibrations inferable from slight underlying changes, as well as aiding the investigation of functional groups in geopolymers. The essential band of clay based geopolymers is located at around 990 cm<sup>-1</sup>, which is related to the deviated extending/asymmetric stretching of silicon and oxygen bonds and aluminium oxygen links.<sup>62,113</sup> As the polycondensation cycle advances, the intensity of this band increases, which means an increase in Al<sub>2</sub>SiO<sub>5</sub> in the lattice/matrix. Moreover, because of the higher calcination temperature, it shifts to a higher wavenumber. This is attributed to the substitution of aluminum for silicon, which causes atomic primary adjustments.<sup>114</sup> The progress of Gel 1 to Gel 2 proposed<sup>115,116</sup> shows the spectrum changes from lower to upper wavenumbers, as shown in Fig. 22(a) and (b). Besides, geopolymers display a peak at 720 cm<sup>-1</sup>, which is attributed to the Si–O–Si/Si–O–Al extending/stretching.<sup>61,62,96</sup> Other functional groups or absorption bands can be seen at 560 cm<sup>-1</sup> and 690–440 cm<sup>-1</sup>, showing tetrahedral aluminium extending/stretching groups and Si–O–Si/Si–O–Al twisting vibrations, respectively. The enhanced silica content in

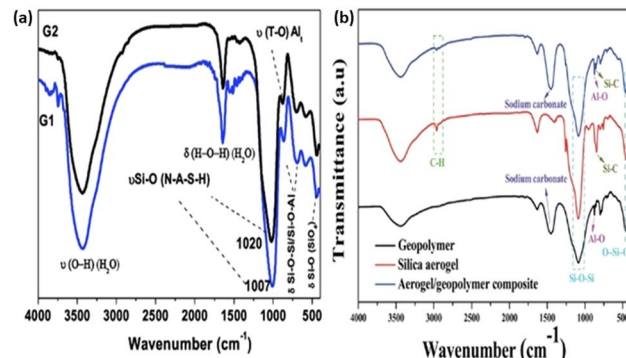


Fig. 22 (a) FTIR spectra of (G1 = Gel 1) and (G2 = Gel2). (b) FTIR spectra of geopolymers, aerogel/geopolymer composite and aerogel.<sup>115,116</sup>

geopolymer structures improves their strength. This is because of the stronger Si–O–Si bonds than Si–O–Al bonds.<sup>117</sup>

## 7. Properties of clay-based geopolymers

Besides their exceptional mechanical and physical properties, geopolymers exhibit low thickness and resistance to heat, fire, and chemicals, and other heat-related hazards. As a result, they are widely used in a variety of fields, such as innovative materials, fireproof materials, and new ceramics. Metakaolin geopolymers are estimated to have a bulk density in the range of 1.20 to 1.80 g cm<sup>-3</sup>. Geopolymers can also be used to create lightweight objects. Their reported bulk density is lower than that of OPC concrete and almost as low as geopolymers made from fly ash and slag. The traditional Portland cement paste, for instance, has a density of >1.80 g cm<sup>-3</sup>,<sup>47</sup> whereas coal fly ash geopolymers have a bulk density ranging from 1.40 g cm<sup>-3</sup> to 1.80 g cm<sup>-3</sup>.<sup>118,119</sup>

The curing conditions, as well as a combination of other factors including the type of geopolymers, alkali concentration, and the nature of soluble base metal silica (SiO<sub>2</sub>), affect the bulk density. With an increase in the curing temperature, the bulk density of geopolymers decreases.<sup>113</sup> The compressive strength of a material corresponds to its mass thickness. Potassium-based metakaolin geopolymers (1.38 to 1.82 g cm<sup>-3</sup>) and sodium-based metakaolin geopolymers (1.24 to 1.71 g cm<sup>-3</sup>) exhibited almost the same density values. Geopolymers based on Na are generally lighter than that based on K. This is because potassium-based geopolymers have a high density and less openings, as recently reported.<sup>74</sup>

Geopolymers set rapidly. Metakaolin geopolymers set and solidify in around 24 h. De Silva *et al.*<sup>37</sup> reported a short setting period of 4 h at a restoring or curing temperature of 40 °C. Compared to metakaolin geopolymers, fly ash geopolymer glue sets and solidifies more rapidly. As indicated by Hardjito *et al.*,<sup>121</sup> this can be achieved in 2 h when cured at 65 °C and 80 °C. Indeed, the curing temperature significantly affects the setting time. Geopolymers set quicker at higher temperatures. The geopolymerization strategy required 4 h at 50 °C. Besides, at

85 °C and 95 °C, the geopolymization cycle required 1.5 and 0.5 h, respectively.<sup>17</sup> If the geopolymer glue is cured at temperatures below the surrounding/ambient temperature, it may take more than one day to set. Rovnanik<sup>113</sup> observed that the strength of geopolymers did not degrade after 28 days, where they required an extended treatment time. De Silva *et al.*<sup>37</sup> observed that a high  $\text{SiO}_2/\text{Al}_2\text{O}_3$  proportion in the underlying synthesis prompts delayed setting and solidifying, as shown in Fig. 23(a). Despite the fact that the setting time was longer, metakaolin geopolymers with a silica to alumina ratio of 3.8 gained higher and more stable strength at a later period, while in the case of the fly ash-based geopolymer, the highest compressive strength after 7 days was obtained at the  $\text{SiO}_2/\text{Al}_2\text{O}_3$  ratio of 4.18, as shown in Fig. 23(b).<sup>120</sup> The setting time was quick when the  $\text{Al}_2\text{O}_3$  fixation was high; notwithstanding, assuming that the  $\text{SiO}_2$  content is low, the strength will endure. Moreover, the "Ca" content in the precursor material has a huge impact on the setting time. This is based on the fact that the presence of calcium offers more nucleation sites for the precipitation of degraded species, resulting in a faster setting and solidifying speed.<sup>122</sup> After just 4 h at 20 °C, the geopolymers exhibited a compressive strength of 20 MPa. The 28 days compressive strength of geopolymers may be as high as 70 to 100 MPa.<sup>1</sup> An increase in strength shows that the source materials break down more effectively or more rapidly, generating more aluminosilicate species, which are the main components in the geopolymization interaction. The compressive qualities of geopolymers can straightforwardly be determined by the activation degree of the source materials. Geopolymers are not entirely characterized by their gel phase strength, how much gel phase is created, and the amorphous nature of the reaction products.<sup>85</sup> Geopolymers offer extraordinary stability to heat with simply 2% shrinkage. Geopolymers have a ceramic-like design and are steady up to 1000–1200 °C.<sup>10,34,65,123</sup> Geopolymers are correspondingly steady in their functioning in the range of 250 °C and 800 °C, according to Subaer and van Riessen. Filler (for example  $\text{SiO}_2$  or rock) and foaming agents (for example ground aluminium and  $\text{H}_2\text{O}_2$ ) were added to geopolymers during blending to enhance their thermal characteristics. An increase in the content of quartz or rock in the blend diminished the shrinkage to 1%.<sup>33</sup> Besides, according to researchers,<sup>35</sup> foamed geopolymers supported with  $(\text{C}_3\text{H}_6)_n$  strands have flame resistance for around 60 min, as

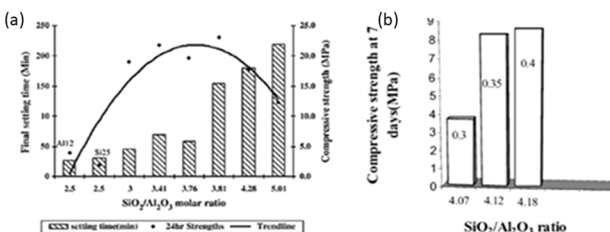


Fig. 23 (a) Compressive strength and final setting time of metakaolin geopolymers with constant  $\text{H}_2\text{O}/\text{Na}_2\text{O}$  molar ratio of 13.6 and varying  $\text{SiO}_2/\text{Al}_2\text{O}_3$  ratios. (b) Compressive strength of geopolymers with varying  $\text{SiO}_2/\text{Al}_2\text{O}_3$  ratios.<sup>37,120</sup>

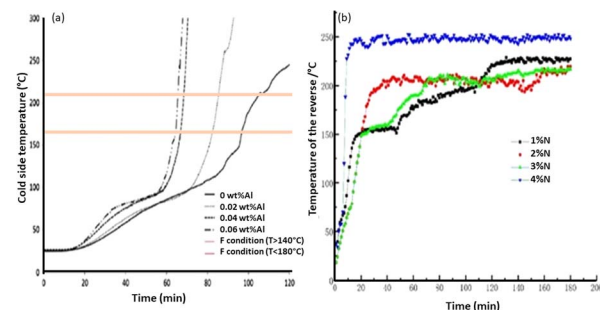


Fig. 24 (a) Fire testing of 4 different mixtures of metakaolin geopolymers. (b) Fire resistance test of metakaolin geopolymers activated with  $\text{Na}_2\text{O}_2$ ; N shows percentage of  $\text{Na}_2\text{O}_2$ .<sup>35,124</sup>

shown in Fig. 24(a). Foamed geopolymers have great potential for use as warm protector/thermal insulators in the environment considering their low thickness and compressive strength. To achieve a comparative fire rating, materials should have exceptionally low thermal conductivity and thermal damage resistance. Elimbi *et al.*<sup>39</sup> found that when metakaolin geopolymers heated in the range of 300 °C and 900 °C, their uniformity/strength decreased. This was ascribed to the slow progress of the geopolymer framework transforming into translucent phases. At 1000 °C, the metakaolin geopolymers extended and broke, as shown in Fig. 24(b).

Under acidic and antacid/alkaline conditions, geopolymers have high toughness.<sup>111,125</sup> In experiments, they were found to be stronger under alkaline conditions. When submerged in ocean water (potential of hydrogen = 8) and  $\text{Na}_2\text{SO}_4$  arrangement (5% sodium sulfate) for a full year, their mechanical properties not degrade. However, geopolymers were fundamentally damaged when lowered in HCl solution for a long period. With an increase in applied test mass, their pressure strength diminished. This was undoubtedly caused by the de-aluminization of the geopolymer structure in an exceptionally acidic environment. Because of the breakage of the Si–O–Al bonds, de-aluminization causes mass loss in the geopolymer structure, generating more corrosive silicic particles in the corrosive media. Subsequently, the microstructure of the geopolymers became more permeable or porous, as shown in Fig. 25(a) and (b).<sup>126,127</sup>

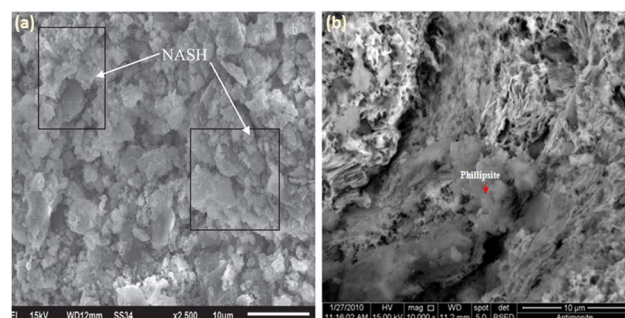


Fig. 25 (a) SEM image of fly ash-based geopolymer exposed to acid attack for 365 days. (b) SEM image of kaolinite geopolymer exposed to acid attack for 90 days.<sup>126,127</sup>



Drying shrinkage happens when unbound water is lost during curing, causing the geopolymer grid to contract. As recently expressed, adding filler to geopolymers reduces their shrinkage. Generally, materials with a higher convergence of better components/finer components will contract more than that with a high content of coarser materials.<sup>35</sup> The drying shrinkage of geopolymers with sand filler, for instance, was 0.01% after 180 days. In contrast, the drying shrinkage of geopolymers without sand filler changed somewhere in the range of 0.03% to 0.04%.<sup>126</sup>

## 8. Factors affecting the properties of clay-based geopolymers

Geopolymer growth is influenced by a variety of factors, including the initial solid or fluid substance, molecule size, the number of reactive stages, the substance organization/chemical composition, type of  $\text{Al}_2\text{SiO}_5$ , type of metal silicate, alkali concentration, curing systems (curing regimes), fillers or added substance content, and water content.

### 8.1 Concentration of alkali

The mechanical and physical characteristics of geopolymers are significantly influenced by alkali substances. Soluble alkali increases the dissolution and disintegration of aluminosilicates, as well as the rate of geopolymerization.<sup>38</sup> However, the amount of particles expected to dissolve by the soluble alkali is still under debate, which is pH dependent. As a rule, an increase in the concentration of NaOH in the range of 4–12 M fortifies metakaolin geopolymers. XRD examination uncovered that the quantity of shapeless phases increased with an increase in the concentration of NaOH, as shown in Fig. 26(a) and (b).<sup>97,128</sup> The heat activation increased as the alkali/antacid concentration increased. Thus, the ideal alkalinity for the disintegration of the source materials is recommended to achieve a higher heat activation rate.<sup>38,94</sup> The  $\text{Na}^+$  particle and OH will be connected during the cycle. Thus, there will be a lack of OH to totally break down  $\text{Si}^{4+}$  and  $\text{Al}^{3+}$  from the aluminosilicates in examples with a low sodium concentration, as well as inadequate  $\text{Na}^+$  to achieve total geopolymerization. Thus, the obtained geopolymer

had poor compressive strength.<sup>59</sup> Despite the prior finding, various researchers concurred that excessive alkalinity diminishes the strength of geopolymers. The strength of geopolymers increases with an increase in the concentration of NaOH solution and diminishes once it reaches the ideal/optimum value. As indicated by Zuhua *et al.*,<sup>94</sup> the best NaOH concentration for the creation of metakaolin geopolymers is 9 M. The polymerization response is unsatisfactory over this ideal value. Given that a high convergence of sodium hydroxide arrangement is sticky, it may impede the leaching of silicon and aluminium from the  $\text{Al}_2\text{SiO}_5$  sources, resulting in the untimely precipitation of geopolymer gels and poor mechanical properties in the final product, which is attributed to the unreacted precursor material.<sup>129</sup> Compared to the study by Alonso and Palomo,<sup>61</sup> increasing the NaOH concentration reduces the polycondensation interaction, as shown in Fig. 27(a) and (b). The concentration of NaOH utilized (10–18 M) was marginally higher than that in other studies. An increase in NaOH concentration was observed to limit polymerization given that numerous degraded particles in a basic arrangement produced immersion/saturation, which confined/restricted the interaction between the polymerized species and the formation of coagulated designs.<sup>13,61</sup> Singh *et al.*<sup>130</sup> confirmed this, expressing that a high alkaline environment with an increase of more than 30 mol% of complete  $\text{Na}_2\text{O}$  is not suggested. Similarly, the speed of geopolymerization is supposed to be related to the pace of geopolymer setting. Metakaolin geopolymers did not set in 6 M of NaOH, according to Steveson and Sagoe-Crentsil,<sup>71</sup> but flash set in 13 M NaOH. With an increase in the antacid/increasing alkali concentration (7–12 M), geopolymers become denser and have a smoother surface. The enhancement in strength is related to this. Quick setting is facilitated by a high antacid/alkali concentration, which shortens the time for disintegration and reduces the amount of unreacted material at the end. An increase in the concentration of NaOH has been connected to a longer setting time. In this case, a blast heater/furnace slag and potassium hydroxide system was used, with the clarification that potassium hydroxide reduces the sticky behaviour of the geopolymer framework.<sup>131</sup> Likewise, the functionality of geopolymers changes depending on the alkali concentration used. As recently expressed, an increment in alkali concentration caused geopolymers to set at a faster rate, which is associated with the effectiveness of the paste. Overall,

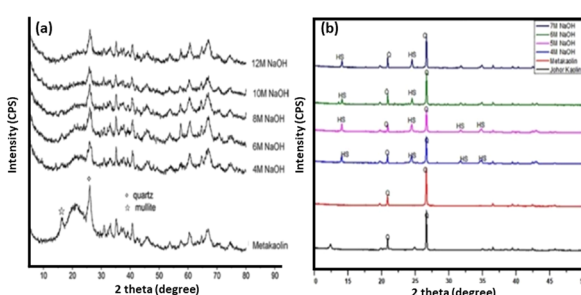


Fig. 26 (a) XRD patterns of metakaolin geopolymers made with different NaOH concentrations and cured at a temperature of 20 °C for 1 h, and then cured for 10 h at a temperature of 65 °C. (b) XRD patterns of Johor kaolin, metakaolin and hydrosodalite with 4 M, 5 M, 6 M and 7 M NaOH.<sup>97,128</sup>

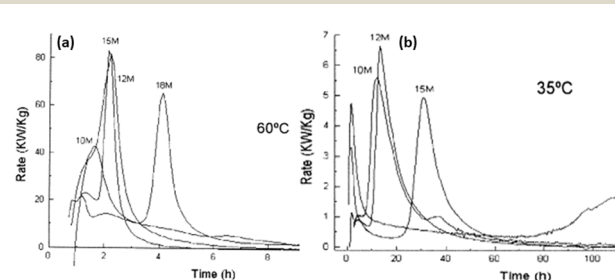


Fig. 27 (a) Calorimetric curves of calcium hydroxide used with metakaolin geopolymers. (b) Curves showing heat evolution of geopolymers activated with NaOH solution.<sup>61</sup>



increasing the alkali content reduces the paste functionality of geopolymers. The impact of soluble base activation on the usefulness of metakaolin geopolymers has gotten little consideration. Increasing the concentration of fly ash geopolymers decreased their functionality.<sup>129,132</sup> Both low and high antacid/alkali concentrations/fixations have been connected to low compressive strength. This may likewise be found in a geo-polymer framework made of fly ash and slag.<sup>131,133</sup> It is essential that the soluble alkali concentration should be sufficiently high to charge-balance the geopolymer networks; however, not too high to cause the creation of  $\text{Na}_2\text{CO}_3$  through carbonation.<sup>134</sup>

## 8.2 Solid/liquid ratios

The solid content refers to  $\text{Al}_2\text{SiO}_5$  during the formation of geopolymers, while the fluid substance refers to the alkali reactant. The solid to liquid proportion is critical considering the fact that it controls how much solids and fluids are utilized in homogeneous blending, which straightforwardly affects the functionality, disintegration, geopolymerization response, and finally the uniformity/strength of the product. Overall, for clay geopolymers, especially metakaolin geopolymers, the ideal S/L proportion is 0.80.<sup>18,94,135</sup> The S/L proportion fundamentally affects the geopolymer paste function, which was diminished when the S/L proportion expanded/increased. S/L proportions greater than 2.0 brought restricted the usefulness of metakaolin geopolymers, as indicated by Yao *et al.*<sup>38</sup> Alternatively, a low S/L proportion reduces/slow down the geopolymerization response. With an increase in the S/L proportions, Fernandez-Jimenez<sup>136</sup> observed a comparative usefulness pattern for fly ash geopolymers. Fly ash geopolymers can endure a more noteworthy S/L proportion. As a result of the wide distance between molecules and less molecule impedance/interference, a medium with a high liquid proportion (low solid to liquid proportion) limits the molecule to-molecule contact of the precursor materials, affecting the functionality of geopolymer paste.<sup>29</sup> Due to usefulness/workability limits, an indistinguishable S/L (solid to liquid) proportion for both fly ash and metakaolin geopolymers will never be achieved. It is important to realize that the use of fine raw materials have an influence on the amount of water used. Metakaolin requires more fluid than fly ash. This is evident from the differences in molecular structure between metakaolin and fly ash; metakaolin has a layered pattern, whereas fly ash has a round form/structure. The multilayer construction limits molecule versatility during blending, making it less serviceable. To acquire uniform blending, metakaolin geopolymers require lower solid to liquid proportions than fly ash geopolymers. In the synthesis of metakaolin and fly ash geopolymers, for instance, Kong and co-workers<sup>18</sup> proposed solid to liquid proportions between 0.8 and 3, individually. The void volume and porosity in geopolymer, and consequently the strength of the final product, are straightforwardly impacted by the functionality of the glue/paste.<sup>52</sup> According to Zuhua *et al.*,<sup>94</sup> a lower S/L proportion results in quick aluminosilicate disintegration. Despite the fact that increasing the concentration of sodium hydroxide enhanced the aluminosilicate draining/leaching, it was

restricted by diminishing the polycondensation cycle at a very high concentration, as depicted previously. Regardless, more noteworthy S/L proportions of 3 (ref. 97) have been seen previously, and some have contended that the S/L proportion should be in the range of 1 to 5.<sup>137</sup>

## 8.3 Alkali reactant ratios

Geopolymers require a certain ratio of sodium hydroxide solution to liquid sodium silicate solution. This is due to the fact that NaOH acts as a dissolvent in the geopolymerization reaction, whereas  $\text{Na}_2\text{SiO}_3$  functions as a fastener/binder. In light of previous study, a large range of  $\text{Na}_2\text{SiO}_3/\text{NaOH}$  ratios remains unknown, from 0.24 to 2.2. In the case of metakaolin geopolymers with an extreme compressive strength of  $59 \text{ N mm}^{-2}$ , Wang *et al.*<sup>97</sup> proposed an  $\text{Na}_2\text{SiO}_3/\text{NaOH}$  proportion of 0.24. Pelisser *et al.*<sup>138</sup> made metakaolin geopolymers utilizing a larger range of  $\text{Na}_2\text{SiO}_3/\text{NaOH}$  proportions (1.0, 1.6, and 2.2). At 1.6, the greatest strength (64 MPa following 7 days) was achieved. The lowest strength was observed with a proportion of 1 and a permeable geopolymer grid, as shown in Fig. 28(a) and (b). The above-mentioned result was supported by Poowancum and co-researchers<sup>139</sup> for a geopolymer made with calcined clay particles. In any case, while utilizing sedimentary clay, the best proportion was viewed as 0.50, with a strength of  $27 \text{ N mm}^{-2}$ , as shown in Fig. 29(a) and (b). The strength of clay sediment geopolymers is weaker than metakaolin geopolymers, which is likely due to the weak reactivity of clay sediment when compared to metakaolin. It was anticipated that at 1.0, there would be deficient NaOH and  $\text{Na}_2\text{SiO}_3$  for full disintegration and binder formation/folio development, as shown in Fig. 29(a) and (b), respectively. The strength of geopolymers is enhanced when the alkali reactant proportion increases. The polymerization cycle is promoted with an increase in the  $\text{Na}_2\text{SiO}_3$  concentration, resulting in enhanced mechanical strength in the item/final product.<sup>41</sup> The degree and speed of the geopolymerization based on the soluble alkali reactant proportions is still under debate.<sup>73</sup> Nonetheless, at a specific high proportion, the usefulness of the glue is restricted, resulting in a decrease in strength.

Pinto claimed that metakaolin geopolymers could not be joined at a proportion under 0.85. This is most likely owing to the viscosity of liquid  $\text{Na}_2\text{SiO}_3$ , which results in a tacky geopolymer

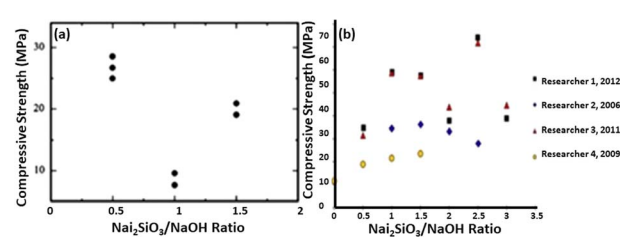


Fig. 28 (a) Graph showing the relationship between molar ratio of alkali reactants and compressive strength. (b) Graph showing the relationship between compressive strength and ratio of alkali reactant with the NaOH concentration of 10 M.<sup>139</sup>



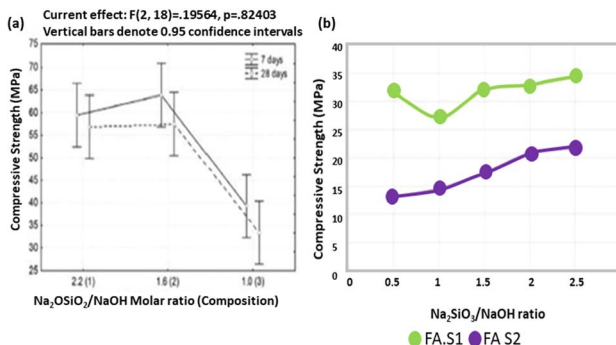


Fig. 29 (a) Relationship between ratio of alkali reactant and compressive strength of sedimentary clay geopolymers. (b) Relationship between alkali reactant ratios and compressive strength by different researchers.<sup>140,141</sup>

glue.<sup>29</sup> The strength development of zeolite geopolymers is helped by increasing the  $\text{Na}_2\text{SiO}_3/\text{NaOH}$  proportion to 1.5.<sup>24</sup> It is basic to recall that the antacid/alkali reactant proportion is not determined by the usefulness of the geopolymer combination, where in the case of clay geopolymers, a more modest and lower soluble alkali reactant proportion range is regularly utilized. Alkali reactant proportions of 0.05–3.00 and 0.40–2.50 have been utilized for fly ash geopolymers.<sup>136,142,143</sup> This is attributed to the way that round particles decrease the molecule grinding<sup>144</sup> and diminish the surface-to-volume ratio,<sup>145</sup> enhancing the functionality of the blends.

The alkali reactant proportion may be expressed as a molar proportion of  $\text{SiO}_2/\text{Na}_2\text{O}$ . Increasing the  $\text{SiO}_2/\text{Na}_2\text{O}$  proportion reverses the cycle/slow the process and makes the glue set later. The response pace of a framework with an Na-silicate solution is slower than that of a framework with K-silicate solution.<sup>73</sup> To achieve further developed strength and sturdiness, Davidovits<sup>67</sup> suggested an  $\text{SiO}_2/\text{Na}_2\text{O}$  proportion of 1.85 for basic reactants. Table 3 presents the molar ratios of oxides recommended by Davidovits.<sup>146</sup>

Higher alkali reactant proportions resulted in the formation of geopolymers with more unreacted particles, as indicated by Duxson *et al.*,<sup>117</sup> while lower alkali reactant proportions created a gel microstructure. Huge quantities of little labile species such as  $(\text{Si}_2\text{O}_5^{2-})_n$ ,  $\text{AlO}_3^{1-}$  monomer, and  $\text{Al}_2\text{SiO}_5$  dimer were anticipated to be available in metakaolin geopolymers created utilizing arrangements with a low  $\text{SiO}_2/\text{M}_2\text{O}$  molar proportion of 0.50 throughout the framework. For a higher  $\text{SiO}_2/\text{M}_2\text{O}$  molar proportion of “1”, a large percentage of the aluminium released

Table 3 Recommended molar ratios of oxides

Molar proportion of different oxides	Range
$\text{H}_2\text{O}/\text{Na}_2\text{O}$	15–17.50
$\text{Na}_2\text{O}/\text{SiO}_2$	0.20–0.28
$\text{Na}_2\text{O}/\text{Al}_2\text{O}_3$	0.80–1.20
$\text{SiO}_2/\text{Al}_2\text{O}_3$	3.50–4.50

after disintegration was projected to be consolidated in the geopolymer network. However, NaOH pellets are less expensive than liquid sodium silicate. As a result, it is advantageous to employ a low alkali reactant percentage in the geopolymer system without affecting the utility and strength of the resulting product.

#### 8.4 Molar ratios (sodium, aluminium, silicon and water contents)

The molar ratio of elements plays an important role in the geopolymer framework. The Na content of the geopolymer framework is resolved using fluid  $\text{Na}_2\text{SiO}_3$  and NaOH.  $\text{Al}_2\text{SiO}_3$  and fluid  $\text{Na}_2\text{SiO}_3$  increase the Si content, while  $\text{Al}_2\text{SiO}_3$  alone increases the Al content. The NaOH arrangement, fluid  $\text{Na}_2\text{SiO}_3$ , and free water introduced in the mixing system all increase the  $\text{H}_2\text{O}$  concentration. In the geopolymer framework, varying the mixing parameters (such as NaOH concentration, S/L ratio, and  $\text{Na}_2\text{SiO}_3/\text{NaOH}$  ratio) results in different atomic or oxide molar ratios. However, the reaction or recovery phases of  $\text{Al}_2\text{SiO}_3$ , the time available, and the extent to which they are consolidated to create a rigid organization/rigid network all influence the amount of each element present in the geopolymerization reaction.

The fundamental elements of Si, Al, and Na limit the amorphous-crystalline phase change,<sup>37,50</sup> as shown in Fig. 30(a) and (b). The most essential proportions are Si/Al and Na/Al. To achieve high strength and toughness, Davidovits advised that

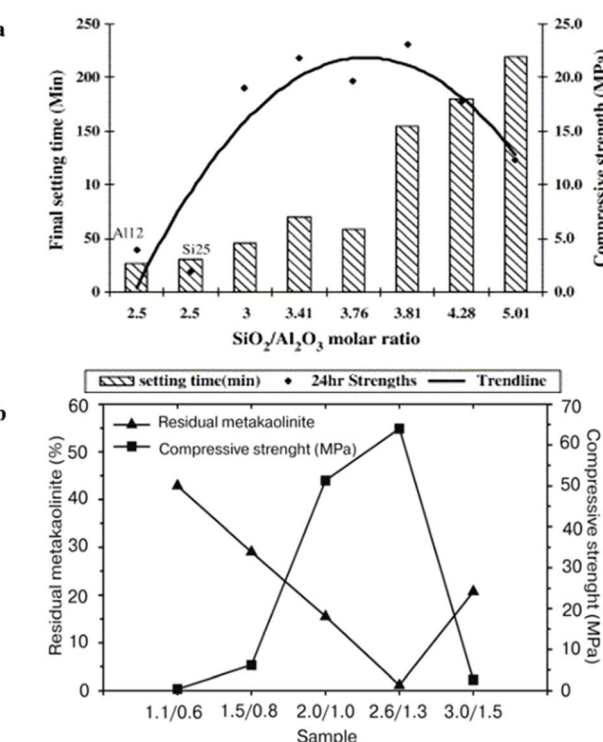


Fig. 30 (a) Compressive strength and residual metakaolin concentration in geopolymers at different  $\text{Si}:\text{Al}/\text{Na}:\text{Al}$  ratios, as calculated using MAS spectra. (b) Flexural strength and compressive strength of geopolymers at various  $\text{Si}/\text{Al}$  ratios.<sup>37,50</sup>

the structure of geopolymers be within the range described in Table 3. Based on this, he determined that the optimal  $\text{Na}_2\text{O}/\text{Al}_2\text{O}_3$  and  $\text{SiO}_2/\text{Al}_2\text{O}_3$  ratios are 1.00 and 4.00, respectively. The Si/Al ratio influences geopolymer disintegration, hydrolysis, and build-up reactions.<sup>147,152</sup> However, most studies reported optimal  $\text{SiO}_2/\text{Al}_2\text{O}_3$  ratios of 3–3.8 based on previous studies, which are significantly lower than the range represented in Table 3 and Fig. 30(a), (b).<sup>37,50,80</sup>

The mechanical characteristics are improved by expanding the  $\text{SiO}_2/\text{Al}_2\text{O}_3$  proportions.<sup>81,148</sup> The mechanical strength of geopolymers is mostly determined by their silica content, whereas the parameters of geopolymers are limited by the alumina concentration. This can be attributed to the increased disintegration of aluminosilicates towards geopolymerization reactions with an increase in the Si concentration.<sup>38,45,88</sup> An increase in the Si to Al and Na to Al ratios increases the mechanical strength of geopolymers, while also transforming them into a more homogeneous structure.<sup>59</sup>

According to previous reports,<sup>37</sup> increasing the (silica ( $\text{SiO}_2$ )/alumina ( $\text{Al}_2\text{O}_3$ )) ratio from 2.5 to 3.80 increased the initial strength of metakaolin geopolymers with a specified (water ( $\text{H}_2\text{O}$ )/sodium oxide ( $\text{Na}_2\text{O}$ )) ratio of 13. Satisfactory strength of 22 MPa was obtained by using a silica ( $\text{SiO}_2$ )/alumina ( $\text{Al}_2\text{O}_3$ )

ratio of 3 to 3.80 and a sodium oxide ( $\text{Na}_2\text{O}$ )/alumina ( $\text{Al}_2\text{O}_3$ ) ratio of about “1.00”, as shown in Fig. 31(a)–(d).<sup>71</sup> Duxson *et al.*<sup>117</sup> also investigated these ideal ratios, achieving a maximum strength of around 80 MPa. Alternatively, Provis and van Deventer<sup>149,150</sup> discovered that increasing the silica ( $\text{SiO}_2$ )/alumina ( $\text{Al}_2\text{O}_3$ ) ratio from 2 to 3.5 decreased the initial reaction speed of geopolymerization due to binder solidification. Their research focused on the response kinetics and made no mention of strength. In another studies,<sup>114,147,150</sup> demonstrated that the building cycle of geopolymer frameworks with low Si/Al fractions occurs mostly between the aluminate and silicate species, resulting in poly(sialate) structures. Poly(sialate-siloxo) and poly(sialate-disiloxo) geopolymer structures were observed in geopolymer frameworks with high Si/Al proportions as a consequence of controlling the build-up communication between silicate species, generating oligomeric silicates that react with  $\text{Al}(\text{OH}_4)_4$ . Poly(sialate) has less siloxo Si–O units than poly(sialate-siloxo) and poly(sialate-siloxo), as seen in Fig. 32(a) and (b). The durability was boosted by increasing the number of siloxo units. Steveson *et al.*<sup>71</sup> utilized a comparable range of  $\text{SiO}_2/\text{Al}_2\text{O}_3$  proportions. The highest strength (47 MPa) was achieved with a silica/alumina ratio of 3 to 3.89, which is nearly double that reported by De Silva *et al.*<sup>37</sup> Correspondingly, the compressive strength increased as the structure improved to become a better, denser, and mediating geopolymer matrix. The distinction in their examination was a slightly lower water-to-sodium peroxide proportion of 12 and a somewhat high sodium peroxide to alumina proportion of 1.2 in their trials. This demonstrates that the test by Steveson and Sagoe-Crentsil<sup>71</sup> contained more  $\text{Na}_2\text{O}$  (sodium peroxide), resulting in the disintegration of more source materials and length of geopolymer creation/production.

Lizcano *et al.*<sup>74</sup> developed geopolymers with a strength of 34 MPa using a silica to alumina ratio of 3.00, at fixed water to sodium peroxide and sodium peroxide to alumina proportions of 1 and 10, respectively., utilizing a potassium-based alkali reactant system. The size and distribution of breaks, voids, and incorporations will decide the eventual strength of the product. At high Si/Al proportions, lingering/residual metakaolin particles in the lattice act as defects, reducing the strength.<sup>71,117</sup> The thickness and pores of geopolymers are unaffected by the silicon/aluminum proportion.<sup>151</sup> As indicated by Kong *et al.*,<sup>52</sup>

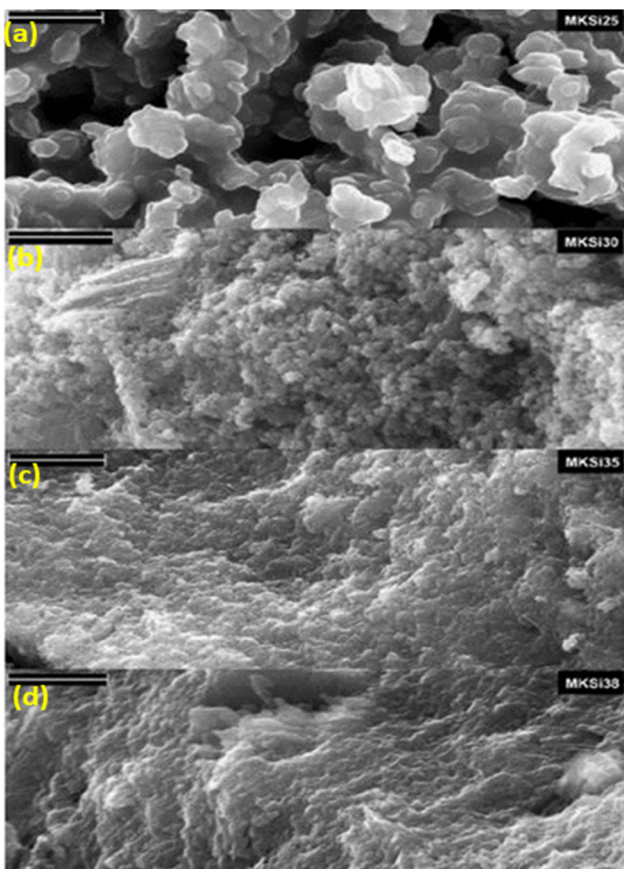


Fig. 31 (a)–(d) High-resolution SEM micrographs of metakaolin with different silica contents (MK = metakaolin, MKSi25– $\text{SiO}_2/\text{Al}_2\text{O}_3$  = 2.5, MKSi30– $\text{SiO}_2/\text{Al}_2\text{O}_3$  = 3.0, MKSi35– $\text{SiO}_2/\text{Al}_2\text{O}_3$  = 3.5, and MKSi38– $\text{SiO}_2/\text{Al}_2\text{O}_3$  = 3.8).<sup>71</sup>

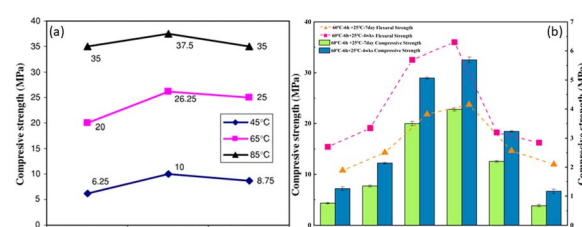


Fig. 32 (a) Compressive strength of pozzolan geopolymers at different  $\text{Na}/\text{Al}$  ratios and cured at different temperatures under hydrothermal treatment (IP1– $\text{Na}/\text{Al}$  = 0.92, IP2– $\text{Na}/\text{Al}$  = 1.08, IP3– $\text{Na}/\text{Al}$  = 1.23). (b) Flexural and compressive strength of geopolymers at different values of  $\text{Na}/\text{Al}$  ratio.<sup>114,147</sup>



the strength decreased when this proportion was increased to 4.6. The outcome changes depending on what was previously disclosed. The degradation was thought to be the result of the increase in strength due to the fact that the silica fume delivered contained more  $\text{Na}_2\text{O}$  (sodium peroxide), resulting in greater disintegration of the source materials and a longer period of geopolymer formation/production. For the preparation of metakaolin geopolymers, scientists utilized uncommonly high  $\text{SiO}_2/\text{Al}_2\text{O}_3$  proportions in a few analyses, and the molar proportion of  $\text{SiO}_2/\text{Al}_2\text{O}_3$  was found.<sup>112,152,153</sup> The best pulverizing strength (10.9 MPa) was achieved when the proportion was 16:1. At a proportion higher than 24, the mechanical strength could not be established. Shockingly, tests with  $\text{SiO}_2/\text{Al}_2\text{O}_3 < 2$  did not properly display the common attributes/characteristics of geopolymers; however, tests with a silica to alumina ratio higher than 24 were run on typical geopolymers, showing elastic rather than brittle behaviour.

Soluble positive alkali ions must be present in geopolymer networks to modify the aluminium anion in the IV-fold coordination. To achieve electrical neutrality, one mole of IV-fold-assisted  $\text{Al}^{3+}$  requires 0.5 moles of sodium peroxide ( $\text{Na}_2\text{O}$ ).<sup>11,19,104</sup> According to most review publications, the justification for optimal strength when  $\text{Na}/\text{Al} = 1$  stems from this. The maximum Si/Al ratio that may be achieved for geopolymers with a sodium to aluminium ratio of 1 is 4.<sup>17,33,117</sup> Riessen,<sup>33</sup> unlike other researchers, discovered that metakaolin remaining in the geopolymer network increased the density, and, hence the durability of the geopolymers. The strength reported by Kani and Allahverdi<sup>114</sup> is displayed in Fig. 32(a). Geopolymers with sodium to aluminum ratios less than 1 have limited advantages, as demonstrated in Fig. 32(b).<sup>114,147</sup>

As recently expressed, this is due to the overabundance of sodium in the geopolymer networks, which negatively affects the geopolymers strength. The level of geopolymerization of dissolved species is constrained by the  $\text{SiO}_2/\text{Na}_2\text{O}$  molar proportion, as shown in Fig. 33(a). An increase in the  $\text{K}_2\text{O}$  or  $\text{Na}_2\text{O}$  concentration resulted in a faster setting rate, improved geopolymer strength development,<sup>154</sup> and decreased breaking/ cracking events.<sup>45</sup> According to Nasab *et al.*,<sup>153</sup> the XRD diffractogram in Fig. 33(b) shows that a high silicate to sodium peroxide proportion (high silicate species) resulted in a bigger

combination of indistinct/amorphous geopolymer phases, while a lower silicate to sodium peroxide proportions resulted in highly crystalline zeolite materials. With a proportion of 2.5 to 3, the geopolymer matrix had more grains and became denser. On account of fly ash geopolymers, Provis *et al.*<sup>155</sup> reported consistent results.

The amount of reaction products generated can be controlled by the alkalinity of the alkali reactant solution in the form of the  $\text{Na}_2\text{O}/\text{H}_2\text{O}$  ratio, which has no effect on the type of final products.<sup>154</sup> In most cases, increasing the  $\text{Na}_2\text{O}/\text{H}_2\text{O}$  ratio improves the clay-based geopolymer dissolution and mechanical strength development.<sup>30</sup> This contradicts the findings by Latella *et al.*,<sup>156</sup> who found that a low water content (water to sodium proportion <5.5) in geopolymers resulted in fractures after 10 days, whereas a water to sodium proportion = 6 resulted in a larger quantity of pores. Steveson and Sagoe-Crentsil<sup>71</sup> found that increasing the  $\text{H}_2\text{O}/\text{Al}_2\text{O}$  ratio from 12 to 16 improved the roughness, number of pores, and intervening geopolymer matrix, as shown in Fig. 34(a)–(c). Anyways, some  $\text{H}_2\text{O}$  must be present in the internal structure of the geopolymer, and the  $\text{H}_2\text{O}$  that was evacuated due to hardening formed holes in the product.

Through a systematic analysis, Yunsheng *et al.*<sup>19</sup> found that the (sodium oxide to alumina) and (water to sodium oxide) molar proportions greatly affected the strength of geopolymer compared to the (silica to alumina) molar proportions. (Silica to alumina ratio) = 5.5, (sodium oxide to alumina ratio) = 1.0, and (water to sodium oxide) ratio = 7.0 resulted in the greatest strength (34.9 MPa). With a (silica to alumina) ratio = 6.3 and (sodium oxide to alumina) ratio 1.1, the strength was considered a totally set geopolymer, which was close to the hypothetical values of a polymer (sialate-disiloxo). Barbosa *et al.*<sup>16</sup> additionally found the ideal conditions of (sodium peroxide to

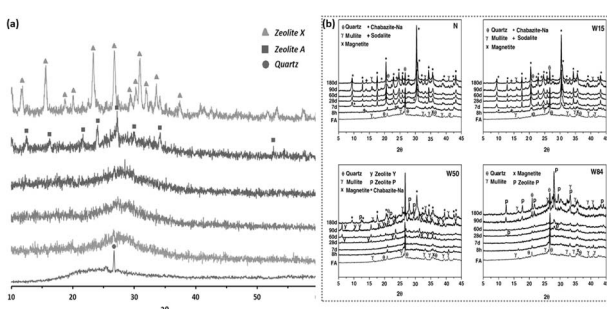


Fig. 33 (a) XRD patterns of metakaolin geopolymers made with different  $\text{SiO}_2/\text{Na}_2\text{O}$  ratios of 2.25, 2.50, 3.00, 3.50, 4.00, and 4.60, and XRD pattern of metakaolin. (b) XRD patterns of fly ash geopolymers with different  $\text{SiO}_2/\text{Na}_2\text{O}$  ratios, for N, W15, W50 and W84 the  $\text{SiO}_2/\text{Na}_2\text{O}$  values are 0, 0.19, 0.69, and 1.17, respectively.<sup>112,153</sup>

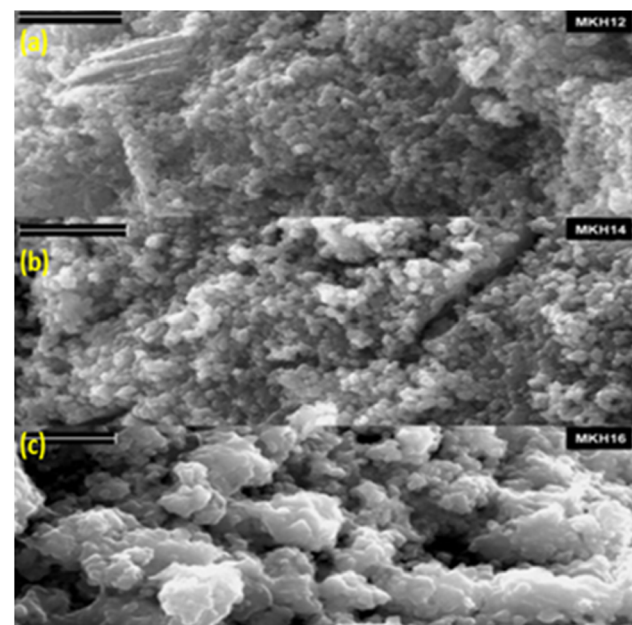


Fig. 34 (a)–(c) SEM images of metakaolin geopolymers at different  $\text{H}_2\text{O}/\text{Al}_2\text{O}_3$  ratios; MKH represents  $\text{H}_2\text{O}/\text{Al}_2\text{O}_3$  (a) 12, (b) 14 and (c) 16.<sup>71</sup>



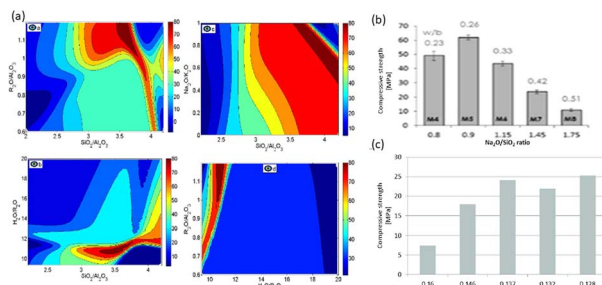


Fig. 35 (a) Effect of various molar ratios ( $R_2O/Al_2O_3$ ,  $SiO_2/Al_2O_3$ ,  $Na_2O/K_2O$  and  $H_2O/R_2O$ ), where ( $R$  = Na or K) on the compressive strength of metakaolin geopolymers shown in a contour plot. The units of contour are in MPa. (b) Graph showing the effect of  $Na_2O/Al_2O_3$  molar ratio on the compressive strength of a geopolymer. (c) Graph showing the effect of  $Na_2O/SiO_2$  molar ratio on the compressive strength of a geopolymer.<sup>157–159</sup>

silica) ratio = 0.25, (water to sodium oxide) ratio = 10, and (silica to alumina) ratio = 3.3. The molar proportion of  $H_2O/Na_2O$  of 25 was found to shape geopolymers with low and immense strength. The geopolymerization response was demonstrated to be reliant on the structure of the blends, mainly their water content. Heah *et al.*<sup>29</sup> found that the best molar ratios of (silica to alumina),  $Na_2O/SiO_3$ , water to sodium oxide, and sodium oxide to alumina for undehydrated kaolin geopolymers were 3.28, 0.28, 14.61, and 0.92, respectively. Regardless of the fact that the observed molar oxide ratios are within the range suggested by Davidovits,<sup>17</sup> the achieved strength was weak and not completely reactive, as evidenced by the huge number of unreacted molecules.<sup>156</sup> Based on the study by Kamalloo *et al.*<sup>157</sup> and the filled contours shown in Fig. 35(a), geopolymers with (potassium oxide to sodium oxide),  $H_2O/M_2O$  ( $M$  = alkali metal),  $M_2O/Al_2O_3$ , and (silica to alumina) ratios of 0.6 to 1, 10 to 11, 1 to 1.2, and 3.6 to 3.8, respectively, had the highest compressive strength (80 MPa). Due to the mixed alkali

effect, they discovered that  $K^+$  cations were better charge balancers in geopolymer structures than  $Na^+$  cations, as shown in Fig. 35(b) and (c).

Specifically, the quantity of Si, Al, and Na in geopolymers considerably affect their definitive qualities. When aluminosilicates other than clay-based were used, the substance shifted/contents varied. Regardless of whether a large portion of the scientists changed the unique combinations, the degree of response determined the final characteristics given that various raw materials have shifting receptive stages and all play a role in forming a rigid network. Analysts found the best oxide molar proportions, as listed in Table 4. Regardless, most of the studies focused on the fact that the combination of geopolymers is restricted to a particular range of Si, Al, and Na contents.<sup>157–159</sup>

## 8.5 Content of water

Water affects the development, design, and attributes of geopolymers. It is a fundamental part of geopolymers. Water serves as a mechanism for oligomer disintegration, particle transport, oligomer hydrolysis, and polycondensation. Zuhua *et al.*<sup>94</sup> portrayed the elements of water during geopolymer arrangement/formation, as shown in Fig. 36. Water additionally works on the flowability of the geopolymer blend. An adequate measure of water helps with blending and offers an instrument for particle transport.<sup>19</sup> The incorporation of extra water during the formation of geopolymers is a cause of stress. Excess water was found to weaken the alkalinity of the framework and move particles/ions from the reaction/response zone.<sup>16,38</sup> Given that geopolymerization is a water-induced response, excess water could hinder the process.<sup>81</sup> The response rate is reduced by high and low water contents, as indicated by Bagheri *et al.*<sup>70</sup> This is believed to be connected with the decrease in hydroxyl ion concentration in the presence of excess water in the system. Interestingly, although the  $OH^-$  concentration decreases at a low water content, the receptive species (monodeprotonated monomer  $H_3SiO_4$ ) for connection between silicate oligomers

Table 4 Outline of ideal molar ratios by researchers

Source material	Molar ratios			Compressive strength	References
	$H_2O/Al_2O_3$	$Na_2O/Al_2O_3$	$SiO_2/Al_2O_3$		
Metakaolin	13.6	1	3–3.81	22 MPa@3 days	37
Metakaolin	54	5	16	10.9 MPa@1 day (crushing strength)	152
Metakaolin	12	1.2	3.9	47 MPa@2 h	71
Metakaolin	10	1	3	34 MPa@1 day (K-based alkali reactant)	74
Metakaolin	—	0.42	3.08	45 MPa@3 days (K-based alkali reactant)	52
Metakaolin	18.01	1.29	5	64 MPa@1 week	50
Metakaolin	10	0.6	3	86 MPa@1 week	33
Natural pozzolan	8.5	0.92	6	45 MPa@1 month	114
Metakaolin	7.2	1	4	70 MPa@10 days (addition of 60% sand)	156
Metakaolin	7	1	5.5	34.9 MPa@1 month	19
Metakaolin	10	0.83	3.3	49 MPa@3 days	16
Kaolin	14.61	0.92	3.28	6 MPa@6 months	29
Metakaolin	10–11	1–1.2	3.6–3.8	80 MPa@1 week	157
Metakaolin	11	1	3–3.8	80 MPa (testing days were not mentioned)	117



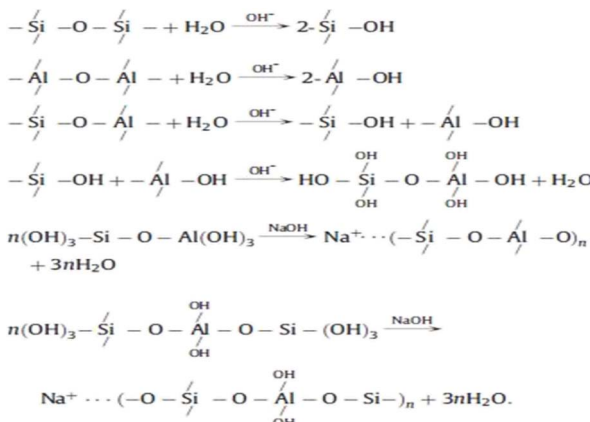


Fig. 36 Contribution/function of water in geopolymer formation.<sup>94</sup>

decreases, slowing the geopolymerization action. The water demand is usually setup/determined by the makeup of the framework. Generally, a low Na/Al proportion requires the utilization of more water. This increasing the risk of breaking during the restoring/curing stage.<sup>160</sup> Moreover, too much water in the geopolymer framework affects the thickness/density and open porosity of the final product. Open porosity is expanded when there is excess water.<sup>151,156</sup>

The water that is lost before drying shrinkage is known as free water, which is trapped in the pores rather than artificially/chemically reinforced. Structural water is characterized as an element of the shrinkage brought about by the geopolymer framework structure. To stay avoid shrinkage, a high starting water content is essential,<sup>161</sup> which considers the extra water to be released before shrinkage starts. To maintain a consistent strength, non-evaporable water must be available in the geopolymer structure (Fig. 37(a) and (b)).<sup>94</sup> Shrinkage and a lack of strength happen because of a deficiency in water during the restoring/curing process.

Nevertheless, the content of water is not determined by the properties of the unrefined components/raw materials used. Moreover, extra blending variables such as soluble base concentration, S/L proportion, and alkali reactant should be considered related to the water content in the geopolymer system/framework.

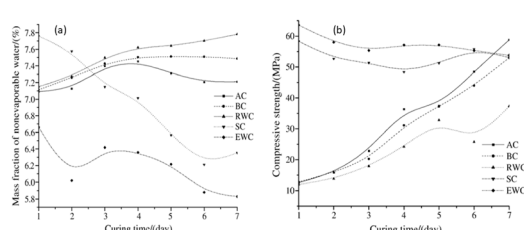


Fig. 37 Under varying curing conditions, variations in (a) non-evaporable water by weight fraction of metakaolin geopolymers and (b) non-evaporable water by weight fraction of metakaolin geopolymers. [AC = in air (22 °C), BC = in a sealed bag (22 °C), RWC = room temperature water (22 °C), SC = in steam (80 °C), and EWC = in hot water (80 °C)].<sup>94</sup>

## 8.6 Curing regime

Subsequent to blending, geopolymers are ordinarily cured at room temperature or somewhat higher. Generally, a temperature of under 100 °C is desirable for curing/restoring. Most scientists agree on this. Davidovits<sup>17</sup> suggested a curing temperature range of 60 °C to 95 °C. Following 4 h of curing at 75 °C, the geopolymer arrangement was almost complete, and the compressive strength of 39.8 MPa was achieved with no further treatment.<sup>13</sup> To acquire enhanced mechanical strength and durability, adequate restoring/curing is generally required.<sup>75</sup> Heat helps the polycondensation cycle and solidifying of the geopolymer matrix by accelerating the disintegration of  $\text{SiO}_2$  and  $\text{Al}_2\text{O}_3$  species from  $\text{Al}_2\text{SiO}_5$  and advancing the disintegration of silica and alumina species from aluminosilicates.<sup>52,61,160,162</sup> Specifically, heat is expected to overcome the heat activation of the cycle and initiate the geopolymerization reaction. Regardless if increasing the curing temperature increases the strength, if the temperature is elevated or the temperature exposure duration is too long, the strength may be reduced. Although a high curing temperature enhances the initial strength, it may compromise the long-term strength.<sup>122</sup> Thermal treatment from 20 °C to 50 °C increased the geopolymerization cycle reaction time, as indicated by researchers<sup>38,163</sup> and shown in Fig. 38(a) and (b). Curing at room temperature consumes a large portion of the day; however, curing at 50 °C does not enhance the strength. This is attributed to the fast formation of the geopolymer structure on the molecule surface, which prevents further aluminosilicate disintegration.<sup>94</sup> At a temperature of 35 no doubt, the ideal conditions are achieved.

According to Rovnanik,<sup>113</sup> higher curing temperatures result in the development of enormous/big openings/holes, which diminishes the strength of geopolymers. The initial and ultimate setting durations of geopolymer slurries were calculated using the Vicat needle method in accordance with the ASTM C191-01 standard. Metakaolin was first combined with an activating solution in a planetary mixer for 5 min to form a homogenous slurry. The produced slurry was then put into a Vicat mold to create the test specimen. In the first setup time measurement, a steel right-cylinder Vicat needle was allowed to pierce the soft specimen, and the penetration depth was measured at regular intervals. The first setting time was

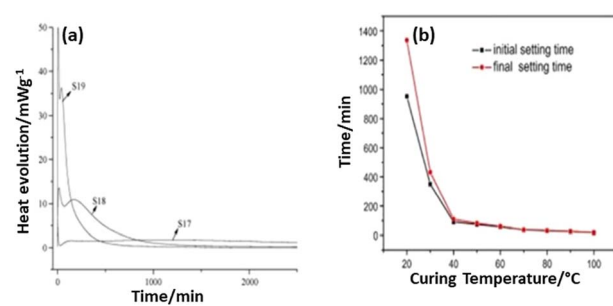


Fig. 38 (a) Effect of curing temperature on geopolymer reaction (S17 = 20 °C, S18 = 35 °C, S19 = 50 °C). (b) Effect of temperature on geopolymer reaction and setting time.<sup>38,163</sup>



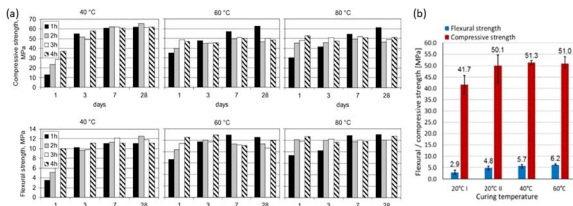


Fig. 39 (a) Data showing effect of curing temperature and time on (top panel) flexural strength and (bottom panel) compressive strength of metakaolin geopolymers. (b) Flexural and compressive strength of metakaolin geopolymers at different curing temperatures.<sup>113,164</sup>

determined as the period between mixing and when the needle penetrated 25 mm into the material, as shown in Fig. 39(a) and (b).<sup>113,164</sup> To calculate the final setting time, the needle test was repeated at intervals until the penetration became minimal, and the final setting time was noted when the needle no longer sunk deeply into the paste. The above-mentioned data were recorded at different curing temperatures, including 20 °C, 30 °C, 40 °C, 60 °C, 80 °C, and 100 °C, to investigate the influence of temperature on the setting behavior of the geopolymer.<sup>38,163</sup> Rovnanik<sup>113</sup> created geopolymer as demonstrated in the referenced figure (Fig. 39(a) and (b)), curing temperature significantly affects the mechanical performance and microstructure of metakaolin-based geopolymers. High-strength goods were obtained by treating at 60 °C and 80 °C; however, the strength was lost after 28 days. Geopolymers cured at 20 °C or 40 °C showed an improvement in strength after being tested for 1 to 28 days. Zuhua *et al.*<sup>94</sup> supported this case. At the point when the geopolymers were treated in water at 20 °C to 22 °C, their strength was poor. This was believed to be caused by the disintegrated species spilling from the geopolymer surfaces.<sup>94</sup> Moreover, high-temperature treatment would certainly improve the breaking capability of geopolymer products. This is because of the quick water loss, which reduces their open porosity.<sup>160</sup> The fast vaporization of blending water prevents the fundamental strength from being created/developed.<sup>77</sup> Thus, sealing the uncovered surfaces of the geopolymer samples during the curing process is proposed. To limit breaking and maintain structural integrity, a small amount of underlying water should be kept in the structure.<sup>31,165</sup> Indeed, even in a fixed climate, water transported and liberated to the outer layer of the geopolymer by narrow activity will prompt a decrease in primary water, according to Zuhua *et al.*<sup>94</sup> Crack-free metakaolin geopolymers were obtained at an ambient and regulated moisture content after a light heat treatment at 40 °C to 60 °C, according to Perera *et al.*<sup>160</sup>

With a change in the curing time, the development of geopolymer design or structures shifts. The structural properties of a geopolymer were evaluated at the curing time of 60 min, 4 h, 2 days, and 3 days at 65 °C, as displayed in Fig. 40 left(a-d) and right(a-d).<sup>166,167</sup> The microstructures revealed the production of an indistinct/amorphous phase and grid/matrix densification as the fix/cure time extended. At 65 °C, the best restoring/curing period was 72 h.<sup>166</sup> At the point when geopolymers based on red

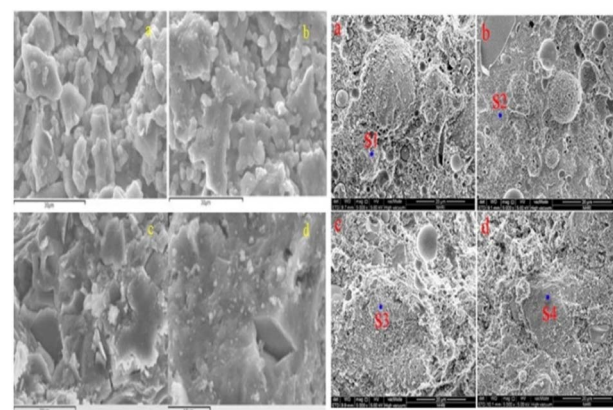


Fig. 40 (Left) (a)–(d) SEM micrographs of geopolymers made of vitreous calcium aluminosilicate that were treated at 65 °C for 60 min, 4 h, 2 days, and 3 days, respectively. (Right) SEM micrograph of fly ash-based geopolymer cement with (a) calcium aluminate = 0%, (b) calcium aluminate = 2.5%, (c) calcium aluminate = 5% and (right) (d) calcium aluminate = 7.5%.<sup>166,167</sup>

mud and rice husk ash aged for 35 days, the compressive strength was almost consistent (11.7 MPa).<sup>162</sup> This meant that the geopolymers would only finish geopolymerization after a certain amount of time had passed.

Kani and Allahverdi<sup>114</sup> focused on a few curing procedures, including steam-saturated aqueous curing and autoclave treatment. The aqueous treatment took less time and was performed at a lower temperature than autoclave curing. Autoclave curing at 210 °C for 30 h after 7 days of pre-curing (25 °C, 95% RH) improved the strength (109 MPa) of the geopolymers with no primary small cracks, as shown in Fig. 41(a) and (b).<sup>114</sup> Curing by electricity helped with reducing the temperature directed by electricity supply, flow, and potential difference, which showed no distinction in eventual outcome strength when contrasted with conventional curing.<sup>168</sup> This could possibly be an alternative approach to restoring. It has been shown that pre-restoring/curing geopolymer glue before typical relieving/curing affects the strength of geopolymers.<sup>114,160,169</sup> The strength result acquired by Kim and Kim<sup>169</sup> is displayed in Fig. 42(a)–(d).<sup>169–171</sup> To make high-strength metakaolin geopolymers, pre-treatment was performed at 75 °C for 3 h, and afterward treatment at ambient temperature for 28 days (51.06 MPa). Pre-treatment is

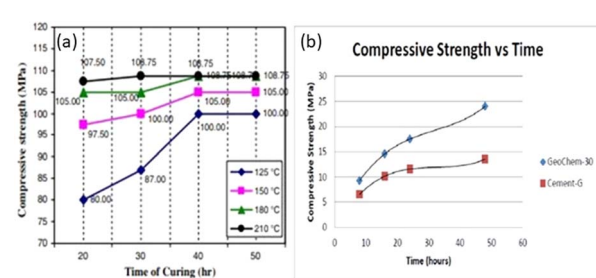


Fig. 41 (a) Compressive strength development of a geopolymer after curing for 7 days at different temperatures. (b) Compressive strength development of a geopolymer with time.<sup>114</sup>

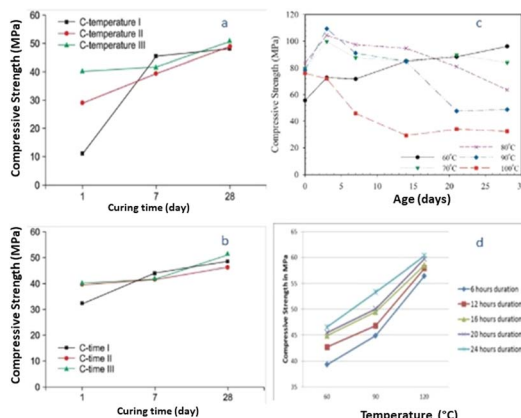


Fig. 42 Impact of (a) pre-relieving temperature and (b) pre-restoring curing time on metakaolin geopolymers compressive strength (C-temperature I-room temperature; C-temperature II-50 °C and C-temperature III-75 °C; C-time I-3 h.; C-time II-6 h.; C-time III-24 h.) (c) Effect of curing time on compressive strength of geopolymers. (d) Effect of curing time on compressive strength of geopolymers.<sup>169–171</sup>

expected for the consistent increase in strength during the thermal treatment process, and great strength can be achieved in the initial phase. Besides, pre-curing diminishes the pores in the geopolymers lattice, considering all the free water remaining in the design/structure.<sup>160</sup> Pre-curing in a muggy climate for a long time prior to thermal treatment is beneficial to enhance the strength, as shown in Fig. 43(a)–(c).<sup>114,172</sup> The synthesis of geopolymers in view of extra aluminosilicate sources, for example, fly ash<sup>136</sup> and regular zeolites,<sup>24</sup> additionally shows a detrimental influence on mechanical strength at a delayed curing time and higher temperature. Clay-based geopolymers, in contrast with fly ash-based geopolymers, require a high-temperature thermal treatment and a more extended curing time to achieve more noteworthy strength geopolymers.

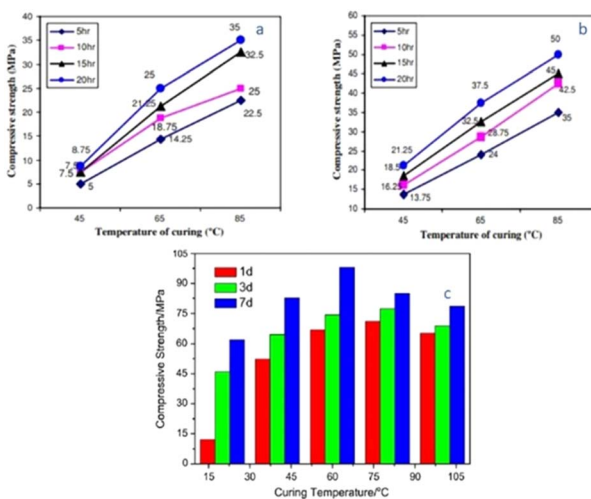


Fig. 43 (a) and (b) Following 1 day and 7 days of pre-curing, the compressive strength of Taftan pozzolan geopolymers was restored under different hydrothermal treatments and (c) effect on curing temperature on geopolymers compressive strength.<sup>114,172</sup>

Nonetheless, this is reliant on the reactivity of the aluminosilicate materials and the natural substance/raw material blending proportions.

For ideal disintegration and accumulation of silica and alumina species, a proper curing system should be utilized. Unacceptable curing conditions (exceptionally low or high temperature) may adversely affect the mechanical attributes/properties of geopolymers.<sup>162</sup> In tuning the strength of geopolymers, the curing temperatures are related to the type and concentration of alkaline reactant solution. Thus, during the synthesis of geopolymers, the curing temperature and term/duration should be coordinated with the soluble base reactant concentration and source material.

## 9. Geopolymers development and applications: past and future

Geopolymers have emerged as a potential class of materials with several applications because of their superior mechanical characteristics, sustainability, and adaptability, as shown in Fig. 44. Their development has been fueled by the demand for economically and environmentally acceptable alternatives to standard cement-based materials, with applications in a variety of industrial sectors. One of the most significant advancements in geopolymers technology has been the invention of outstanding performance binders such as GEOPOLYMIKE and PYRAMENT mixed concrete, which have achieved commercial success in structural engineering for precast and pre-stressed concrete applications. These materials not only provide excellent power, but also help reduce carbon emissions compared to regular concrete.<sup>173</sup>

Besides construction, geopolymers have been used in several other fields. For example, because of their insulating qualities and capacity to tolerate high temperatures, GEOPOLYMIKE binders have been used in combustion linings, tooling, foundry work, and building insulation. Geopolymer-based ceramics

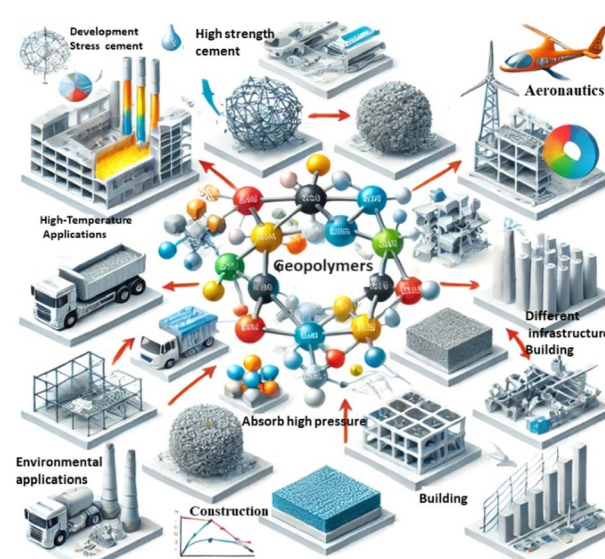


Fig. 44 Different applications of geopolymers.

have also been investigated for their fire and heat resistance, with kaolinite geopolymers being processed at high temperatures to create long-lasting tiles and bricks. Additionally, the use of geopolymer-based materials in aerospace, specifically as fire-resistant composite materials for aircraft interiors, has been a significant milestone.

Geopolymers have also been produced into lightweight concrete products that are simpler to transport and use less energy, in response to the growing need for lightweight materials in structural engineering. These thin geopolymers help with load-bearing applications, in addition to acting as heat insulators. The development of foamed geopolymers has also created opportunities for their application in thermal insulation materials, which makes them appropriate for use in building applications such as home construction. Further increasing their usefulness in building, studies have shown that geopolymer coatings have the ability to reflect heat and provide protection against temperature changes.<sup>174</sup> Geopolymer ceramics are non-ignitable and flame resistant. Besides, a clever way for creating fired materials is to pack geopolymer powder utilizing powder metallurgy and afterward sinter at 1000–1200 °C.<sup>175</sup> Additionally, geopolymers are being investigated for their potential to absorb and immobilize harmful contaminants, which makes them perfect for use in environmental remediation and waste management. Similar to zeolitic materials, they have a special chemical structure that enables them to stabilize and retain harmful chemicals such as heavy metals, making waste disposal safer. To reduce global warming, geopolymers have also been studied for use in cooling systems. Because of their capacity to retain moisture, they are a good fit for evaporative cooling methods. Geopolymers have been evaluated as adhesives and sealants for infrastructure restoration, taking the place of conventional epoxy cements in fiber-reinforced polymer retrofitting. This type of application has demonstrated potential for improving the lifetime and endurance of infrastructure. Their use in acoustic insulation has also been investigated; research has shown that they can be used as materials for sound insulation in building interiors and during construction.<sup>10</sup> In structural design, lightweight substantial materials made of geopolymers have been created because of the requirement for lightweight materials that are simpler to move and consume less energy.<sup>176</sup> Besides, their lightweight concrete capacities, they can be employed as a heat protector and help loading bearing.<sup>177</sup> There have also been examinations on foamed geopolymers in warm protection materials for home structures.<sup>178</sup> Zhang *et al.*<sup>179</sup> utilized geopolymers to make an intelligent and heat-protecting covering. The covering created had 90% reflectivity and warm protection capacity up to 24 °C, on account of the utilization of shades and fillers (for example, titanium dioxide, empty glass microspheres, and powder), as well as a scattering specialist, wetting specialist, and water-holding specialist. Moreover, as reported by Temuujin *et al.*,<sup>180</sup> geopolymers have anti-ultraviolet and anti-aging properties, making them ideal for use as a covering on outside walls to save energy. The examination of geopolymers in heat and fire applications have also been published.<sup>39,181–185</sup> Geopolymers, as recently expressed, have atomic models that are similar to that

of zeolitic materials. Because of their capacity to ingest and harden unsafe synthetic waste, they can immobilize harmful material or weighty metals. This is a favorable strategy for immobilization.<sup>186,187</sup> Extensive research has been done over the years to see if geopolymers can be used in more applications. Okada *et al.*<sup>188</sup> developed porous geopolymers for application in cooling systems. Geopolymers with strong water retention capabilities or slow water release properties inspired this notion. This makes geopolymers appropriate for moisture evaporation-based surface cooling, which aids in reducing global warming resulting from human activities and national growth. Pacheco-Torgal *et al.*<sup>189</sup> reported that geopolymers may be utilized in infrastructure repair. In fiber-reinforced polymer retrofitting, geopolymer glue can be utilized as a sealant for developments and can supplant epoxy cements. Geraldes *et al.*<sup>190</sup> reported a unique review, in which geopolymers were used as tile fix materials. Hung *et al.*<sup>191</sup> depicted the preparation of geopolymers for acoustic protection besides their warm insulative abilities. Geopolymers can be utilized as sound protecting materials in development and structures. The sound decrease coefficient is impacted by the thickness of the geopolymer framework. Scientists have focused on a one-section geopolymer framework<sup>56,57,192</sup> in which a geopolymer blend can be shaped by simply adding water for the utilization of geopolymers in structural designing. The requirement of geopolymer innovation for *in situ* application, which restricts their cost effectiveness, inspired the consideration of this review. Geopolymer research has advanced recently, showing that they can be applied as biomaterials. Pangdaeng *et al.*<sup>122</sup> showed that geopolymers have high bioactivity, which can be improved by the expansion of white Portland concrete. Jämstorp *et al.*<sup>193</sup> and Cai *et al.*<sup>194</sup> investigated the use of a geopolymer as a drug delivery agent. Geopolymers possessing varying pore structures can deliver drugs to target cells.

Despite the major advances in this field, current research has numerous limitations that prevent the complete understanding and practical use of geopolymers. One important problem is variability in experimental methodology, which causes disparities in the reported results due to differences in synthesis processes, processing conditions, and measurement protocols. Furthermore, theoretical models frequently fail to reflect the intricacies of the real-world behavior of materials, reducing their forecast accuracy. Cross-study comparisons are further confounded by discrepancies in sample preparation, characterisation methodologies, and data interpretation, making it difficult to identify globally acknowledged patterns. Thus, to ensure repeatability and dependability, these constraints must be addressed by standardizing experimental frameworks, improving theoretical models, and conducting more thorough comparison investigations. By systematically analyzing these issues, our review enhances the coherence of existing research and provides a clearer direction for future studies.

## 10. Conclusion

This research examined geopolymers and their creation, as well as raw materials, alkali reactant systems, reaction processes,



characterisation, properties/characteristics, and applications, focusing on clay-based geopolymers. This review indicates that regardless of the main material utilized, the geopolymers cycle has comparable component differences in primary material features, such as chemical composition, molecule shape and size, surface area, and contaminants, which may have an influence on the final product. The primary restriction is the layered-like construction of clay-based antecedents/precursors, which results in low reactivity, and consequently low strength geopolymers. Regardless, this is an important topic. Changes to the design of clay materials should be pursued with greater passion. Also, the alkali concentration, blending/mixing proportions and extents, restoring/curing regimes/systems, water content, and the inclusion of added substances/fillers all affect the qualities of geopolymers. The ideal geopolymer is not entirely determined a few blending and handling factors. The primary attributes (soluble base/alkali substance, blending proportions and combination extents, and relieving systems/curing regimes, among others) should be considered to fundamentally affect geopolymers. Geopolymers have been successfully utilized in an assortment of disciplines because of their prevalent characteristics.

## Data availability

No new data were used for the research described in the article.

## Author contributions

All author contributed equally to this article.

## Conflicts of interest

There are no conflicts to declare.

## Acknowledgements

The author are thankful to the Research office of the United Arab Emirates University Al Ain, 1551, UAE.

## References

- 1 J. Davidovits, Geopolymers: man-made rock geosynthesis and the resulting development of very early high strength cement, *J. Mater. Educ.*, 1994, **16**, 91.
- 2 J. Davidovits, Mineral polymers and methods of making them, *US Pat.* 4, 1982.
- 3 K. Ramujee and M. Potharaju, Abrasion resistance of geopolymer composites, *Procedia Mater. Sci.*, 2014, **6**, 1961–1966.
- 4 G. Varga, The structure of kaolinite and metakaolinite, *Epitoanyag*, 2007, **59**(1), 6–9.
- 5 N. Ariffin, M. M. A. B. Abdullah, P. Postawa, S. Zamree AbdRahim, M. R. R. Mohd Arif Zainol, R. P. Jaya, A. Śliwa, M. F. Omar, J. J. Wysłocki and K. Błoch, Effect of aluminium powder on kaolin-based geopolymer characteristic and removal of Cu<sup>2+</sup>, *Materials*, 2021, **14**(4), 814.
- 6 M. Abdullah, L. Y. Ming, H. C. Yong and M. Tahir, Clay-based materials in geopolymer technology, *Cem. Based Mater.*, 2018, **239**, 77438.
- 7 K. Barani and M. Kalantari, Recovery of kaolinite from tailings of Zonouz kaolin-washing plant by flotation-flocculation method, *J. Mater. Res. Technol.*, 2018, **7**(2), 142–148.
- 8 R. A. Al-husseiny and S. E. Ebrahim, Synthesis of geopolymer for the removal of hazardous waste: a review, *IOP Conference Series: Earth and Environmental Science*, 2021, 012102.
- 9 G. Huseien, J. Mirza and M. Ismail, *Theory of geopolymer synthesis*, 2016.
- 10 J. Davidovits, Years of successes and failures in geopolymer applications. Market trends and potential breakthroughs, in *Geopolymer 2002 conference*, Geopolymer Institute Saint-Quentin, France, Melbourne, Australia, 2002, p. 29.
- 11 J. Davidovits, Geopolymers: inorganic polymeric new materials, *J. Therm. Anal. Calorim.*, 1991, **37**(8), 1633–1656.
- 12 J. L. Provis, G. C. Lukey and J. S. van Deventer, Do geopolymers actually contain nanocrystalline zeolites? A reexamination of existing results, *Chem. Mater.*, 2005, **17**(12), 3075–3085.
- 13 D. Khale and R. Chaudhary, Mechanism of geopolymers and factors influencing its development: a review, *J. Mater. Sci.*, 2007, **42**(3), 729–746.
- 14 N. Saidi, B. Samet and S. Baklouti, Effect of composition on structure and mechanical properties of metakaolin based PSS-Geopolymer, *Int. J. Mater. Sci.*, 2013, **3**(4), 145–151.
- 15 J. Davidovits and J. L. Sawyer, *Early high-strength mineral polymer*, Pyrament Inc., Houston, TX, United States, 1984.
- 16 V. F. Barbosa, K. J. MacKenzie and C. Thaumaturgo, Synthesis and characterisation of materials based on inorganic polymers of alumina and silica: sodium polysialate polymers, *Int. J. Inorg. Mater.*, 2000, **2**(4), 309–317.
- 17 J. Davidovits, Mineral polymers and methods of making them, *US Pat.*, US434938A, 1982.
- 18 D. L. Kong, J. G. Sanjayan and K. Sagoe-Crentsil, Comparative performance of geopolymers made with metakaolin and fly ash after exposure to elevated temperatures, *Cem. Concr. Res.*, 2007, **37**(12), 1583–1589.
- 19 Z. Yunsheng, S. Wei and L. Zongjin, Composition design and microstructural characterization of calcined kaolin-based geopolymer cement, *Appl. Clay Sci.*, 2010, **47**(3–4), 271–275.
- 20 J. G. Van Jaarsveld, *The physical and chemical characterisation of fly ash based geopolymers*, 2000.
- 21 J. Temuujin, A. van Riessen and K. MacKenzie, Preparation and characterisation of fly ash based geopolymer mortars, *Constr. Build. Mater.*, 2010, **24**(10), 1906–1910.
- 22 A. I. Bădănoiu, T. H. A. Al-Saadi and G. Voicu, Synthesis and properties of new materials produced by alkaline activation of glass cullet and red mud, *Int. J. Miner. Process.*, 2015, **135**, 1–10.



23 S. Ahmari and L. Zhang, Production of eco-friendly bricks from copper mine tailings through geopolymers, *Constr. Build. Mater.*, 2012, **29**, 323–331.

24 C. Villa, E. T. Pecina, R. Torres and L. Gómez, Geopolymer synthesis using alkaline activation of natural zeolite, *Constr. Build. Mater.*, 2010, **24**(11), 2084–2090.

25 G. Zheng, X. Cui, D. Huang, J. Pang, G. Mo, S. Yu and Z. Tong, Alkali-activation reactivity of chemosynthetic  $\text{Al}_2\text{O}_3$ – $2\text{SiO}_2$  powders and their 27Al and 29Si magic-angle spinning nuclear magnetic resonance spectra, *Particuology*, 2015, **22**, 151–156.

26 K. J. MacKenzie, S. Bradley, J. V. Hanna and M. E. Smith, Magnesium analogues of aluminosilicate inorganic polymers (geopolymers) from magnesium minerals, *J. Mater. Sci.*, 2013, **48**(4), 1787–1793.

27 R. Cioffi, L. Maffucci and L. Santoro, Optimization of geopolymer synthesis by calcination and polycondensation of a kaolinitic residue, *Resour., Conserv. Recycl.*, 2003, **40**(1), 27–38.

28 Z. Zhang, X. Yao, H. Zhu, S. Hua and Y. Chen, Activating process of geopolymer source material: kaolinite, *J. Wuhan Univ. Technol., Mater. Sci. Ed.*, 2009, **24**(1), 132–136.

29 C. Heah, H. Kamarudin, A. M. Al Bakri, M. Bnhussain, M. Luqman, I. K. Nizar, C. Ruzaidi and Y. Liew, Study on solids-to-liquid and alkaline activator ratios on kaolin-based geopolymers, *Constr. Build. Mater.*, 2012, **35**, 912–922.

30 H. Xu and J. Van Deventer, The geopolymerisation of aluminosilicate minerals, *Int. J. Miner. Process.*, 2000, **59**(3), 247–266.

31 J. Van Jaarsveld, J. S. Van Deventer and G. Lukey, The effect of composition and temperature on the properties of fly ash-and kaolinite-based geopolymers, *Chem. Eng. J.*, 2002, **89**(1–3), 63–73.

32 K. J. MacKenzie, D. R. Brew, R. A. Fletcher and R. Vagana, Formation of aluminosilicate geopolymers from 1: 1 layer-lattice minerals pre-treated by various methods: a comparative study, *J. Mater. Sci.*, 2007, **42**(12), 4667–4674.

33 A. Van Riessen, Thermo-mechanical and microstructural characterisation of sodium-poly(sialate-siloxo)(Na-PSS) geopolymers, *J. Mater. Sci.*, 2007, **42**(9), 3117–3123.

34 M. Schmücker and K. J. MacKenzie, Microstructure of sodium polysialate siloxo geopolymer, *Ceram. Int.*, 2005, **31**(3), 433–437.

35 W. D. Rickard, L. Vickers and A. Van Riessen, Performance of fibre reinforced, low density metakaolin geopolymers under simulated fire conditions, *Appl. Clay Sci.*, 2013, **73**, 71–77.

36 W. Guo, G. Wu, J. Wang, Z. Wen and S. Yin, Preparation and performance of geopolymers, *J. Wuhan Univ. Technol., Mater. Sci. Ed.*, 2008, **23**(3), 326–330.

37 P. De Silva, K. Sagoe-Crenstil and V. Sirivivatnanon, Kinetics of geopolymers: role of  $\text{Al}_2\text{O}_3$  and  $\text{SiO}_2$ , *Cem. Concr. Res.*, 2007, **37**(4), 512–518.

38 X. Yao, Z. Zhang, H. Zhu and Y. Chen, Geopolymerization process of alkali-metakaolinite characterized by isothermal calorimetry, *Thermochim. Acta*, 2009, **493**(1–2), 49–54.

39 A. Elimbi, H. Tchakoute, M. Kondoh and J. D. Manga, Thermal behavior and characteristics of fired geopolymers produced from local Cameroonian metakaolin, *Ceram. Int.*, 2014, **40**(3), 4515–4520.

40 F. Pacheco-Torgal, J. Castro-Gomes and S. Jalali, Alkali-activated binders: a review: part 1. Historical background, terminology, reaction mechanisms and hydration products, *Constr. Build. Mater.*, 2008, **22**(7), 1305–1314.

41 F. Pacheco-Torgal, J. Castro-Gomes and S. Jalali, Alkali-activated binders: a review. Part 2. About materials and binders manufacture, *Constr. Build. Mater.*, 2008, **22**(7), 1315–1322.

42 A. Palomo, M. Grutzeck and M. Blanco, Alkali-activated fly ashes: a cement for the future, *Cem. Concr. Res.*, 1999, **29**(8), 1323–1329.

43 E. Güneyisi, M. Gesoḡlu, T. Özturan and K. Mermert, Microstructural properties and pozzolanic activity of calcined kaolins as supplementary cementing materials, *Can. J. Civ. Eng.*, 2012, **39**(12), 1274–1284.

44 H. Wang, C. Li, Z. Peng and S. Zhang, Characterization and thermal behavior of kaolin, *J. Therm. Anal. Calorim.*, 2011, **105**(1), 157–160.

45 H. Xu and J. S. Van Deventer, Geopolymerisation of multiple minerals, *Miner. Eng.*, 2002, **15**(12), 1131–1139.

46 B. R. Ilić, A. A. Mitrović and L. R. Miličić, Thermal treatment of kaolin clay to obtain metakaolin, *Hem. Ind.*, 2010, **64**(4), 351–356.

47 Y. M. Liew, H. Kamarudin, A. M. Al Bakri, M. Luqman, I. K. Nizar, C. M. Ruzaidi and C. Y. Heah, Processing and characterization of calcined kaolin cement powder, *Constr. Build. Mater.*, 2012, **30**, 794–802.

48 A. G. San Cristóbal, R. Castelló, M. M. Luengo and C. Vizcayno, Zeolites prepared from calcined and mechanically modified kaolins: a comparative study, *Appl. Clay Sci.*, 2010, **49**(3), 239–246.

49 I. Lecomte, M. Liégeois, A. Rulmont, R. Cloots and F. Maseri, Synthesis and characterization of new inorganic polymeric composites based on kaolin or white clay and on ground-granulated blast furnace slag, *J. Mater. Res.*, 2003, **18**(11), 2571–2579.

50 M. Rowles, J. V. Hanna, K. Pike, M. E. Smith and B. O'connor, 29Si, 27Al, 1H and 23Na MAS NMR study of the bonding character in aluminosilicate inorganic polymers, *Appl. Magn. Reson.*, 2007, **32**(4), 663–689.

51 P. S. Singh, M. Trigg, I. Burgar and T. Bastow, Geopolymer formation processes at room temperature studied by 29Si and 27Al MAS-NMR, *Mater. Sci. Eng., A*, 2005, **396**(1–2), 392–402.

52 D. L. Kong, J. G. Sanjayan and K. Sagoe-Crenstil, Factors affecting the performance of metakaolin geopolymers exposed to elevated temperatures, *J. Mater. Sci.*, 2008, **43**(3), 824–831.

53 C. Ferone, B. Liguori, I. Capasso, F. Colangelo, R. Cioffi, E. Cappelletto and R. Di Maggio, Thermally treated clay



sediments as geopolymer source material, *Appl. Clay Sci.*, 2015, **107**, 195–204.

54 D. Koloušek, J. Brus, M. Urbanova, J. Andertova, V. Hulinsky and J. Vorel, Preparation, structure and hydrothermal stability of alternative (sodium silicate-free) geopolymers, *J. Mater. Sci.*, 2007, **42**(22), 9267–9275.

55 D. Feng, J. L. Provis and J. S. van Deventer, Thermal activation of albite for the synthesis of one-part mix geopolymers, *J. Am. Ceram. Soc.*, 2012, **95**(2), 565–572.

56 X. Ke, S. A. Bernal, N. Ye, J. L. Provis and J. Yang, One-part geopolymers based on thermally treated red mud/NaOH blends, *J. Am. Ceram. Soc.*, 2015, **98**(1), 5–11.

57 M. X. Peng, Z. H. Wang, S. H. Shen and Q. G. Xiao, Synthesis, characterization and mechanisms of one-part geopolymers cement by calcining low-quality kaolin with alkali, *Mater. Struct.*, 2015, **48**(3), 699–708.

58 B. Nematollahi, J. Sanjayan and F. U. A. Shaikh, Synthesis of heat and ambient cured one-part geopolymer mixes with different grades of sodium silicate, *Ceram. Int.*, 2015, **41**(4), 5696–5704.

59 M. Rowles and B. O'connor, Chemical optimisation of the compressive strength of aluminosilicate geopolymers synthesised by sodium silicate activation of metakaolinite, *J. Mater. Chem.*, 2003, **13**(5), 1161–1165.

60 M. L. Granizo, M. T. Blanco-Varela and S. Martínez-Ramírez, Alkali activation of metakaolins: parameters affecting mechanical, structural and microstructural properties, *J. Mater. Sci.*, 2007, **42**(9), 2934–2943.

61 S. Alonso and A. Palomo, Alkaline activation of metakaolin and calcium hydroxide mixtures: influence of temperature, activator concentration and solids ratio, *Mater. Lett.*, 2001, **47**(1–2), 55–62.

62 S. Alonso and A. Palomo, Calorimetric study of alkaline activation of calcium hydroxide-metakaolin solid mixtures, *Cem. Concr. Res.*, 2001, **31**(1), 25–30.

63 Z. Yunsheng, S. Wei, C. Qianli and C. Lin, Synthesis and heavy metal immobilization behaviors of slag based geopolymer, *J. Hazard. Mater.*, 2007, **143**(1–2), 206–213.

64 A. Buchwald, H. Hilbig and C. Kaps, Alkali-activated metakaolin-slag blends—performance and structure in dependence of their composition, *J. Mater. Sci.*, 2007, **42**(9), 3024–3032.

65 J. Davidovits, *High-alkali cements for 21st century concretes*, Special Publication, 1994, vol. 144, pp. 383–398.

66 C. K. Yip, G. Lukey and J. S. Van Deventer, The coexistence of geopolymeric gel and calcium silicate hydrate at the early stage of alkaline activation, *Cem. Concr. Res.*, 2005, **35**(9), 1688–1697.

67 J. Davidovits and J. Sawyer, Chemistry of geopolymeric system, terminology, *Geopolymer*, 1999, **99**(292), 9–39.

68 C. Panagiotopoulou, E. Kontori, T. Perraki and G. Kakali, Dissolution of aluminosilicate minerals and by-products in alkaline media, *J. Mater. Sci.*, 2007, **42**(9), 2967–2973.

69 O. Vogt, N. Ukrainczyk, C. Ballschmiede and E. Koenders, Reactivity and microstructure of metakaolin based geopolymers: effect of fly ash and liquid/solid contents, *Materials*, 2019, **12**(21), 3485.

70 M. Bagheri, B. Lothenbach, M. Shakoorioskooie, A. Leemann and K. Scrivener, Use of scratch tracking method to study the dissolution of alpine aggregates subject to alkali silica reaction, *Cem. Concr. Compos.*, 2021, **124**, 104260.

71 M. Steveson and K. Sagoe-Crentsil, Relationships between composition, structure and strength of inorganic polymers, *J. Mater. Sci.*, 2005, **40**(8), 2023–2036.

72 J. Phair and J. Van Deventer, Effect of silicate activator pH on the leaching and material characteristics of waste-based inorganic polymers, *Miner. Eng.*, 2001, **14**(3), 289–304.

73 H. Rahier, J. Wastiels, M. Biesemans, R. Willem, G. Van Assche and B. Van Mele, Reaction mechanism, kinetics and high temperature transformations of geopolymers, *J. Mater. Sci.*, 2007, **42**(9), 2982–2996.

74 M. Lizcano, H. S. Kim, S. Basu and M. Radovic, Mechanical properties of sodium and potassium activated metakaolin-based geopolymers, *J. Mater. Sci.*, 2012, **47**(6), 2607–2616.

75 K. Komnitsas and D. Zaharaki, Geopolymerisation: a review and prospects for the minerals industry, *Miner. Eng.*, 2007, **20**(14), 1261–1277.

76 A. Ababneh, F. Matalkah and R. Aqel, Synthesis of kaolin-based alkali-activated cement: carbon footprint, cost and energy assessment, *J. Mater. Res. Technol.*, 2020, **9**(4), 8367–8378.

77 Q. Mohsen and N. Y. Mostafa, Investigating the possibility of utilising low kaolinitic clays in production of geopolymer bricks, *Ceram.-Silik.*, 2010, **54**(2), 160–168.

78 R. R. Lloyd, J. L. Provis and J. S. van Deventer, Microscopy and microanalysis of inorganic polymer cements. 2: the gel binder, *J. Mater. Sci.*, 2009, **44**(2), 620–631.

79 A. M. Al Bakri, H. Kamarudin, M. Bnhussain, I. K. Nizar, A. Rafiza and Y. Zarina, Microstructure of different NaOH molarity of fly ash-based green polymeric cement, *J. Eng. Technol. Res.*, 2011, **3**(2), 44–49.

80 K. Dinesh, I. Sonny, R. Syahrir, C. Davannendran and A. Nuriman, The suitability of fly ash based geopolymer cement for oil well cementing applications: a review, *ARPN J. Eng. Appl. Sci.*, 2018, **13**(20), 8296.

81 J. Davidovits, *Geopolymer Chemistry & Application*, Geopolymer Institute, Saint-Quentin, France, 2008, ISBN 2-951-14820-1-9.

82 S. J. O'Connor and K. J. MacKenzie, Synthesis, characterisation and thermal behaviour of lithium aluminosilicate inorganic polymers, *J. Mater. Sci.*, 2010, **45**(14), 3707–3713.

83 S.-D. Wang, K. L. Scrivener and P. Pratt, Factors affecting the strength of alkali-activated slag, *Cem. Concr. Res.*, 1994, **24**(6), 1033–1043.

84 M. Komljenović, Z. Baščarević and V. Bradić, Mechanical and microstructural properties of alkali-activated fly ash geopolymers, *J. Hazard. Mater.*, 2010, **181**(1–3), 35–42.

85 P. Duxson, A. Fernández-Jiménez, J. L. Provis, G. C. Lukey, A. Palomo and J. S. van Deventer, Geopolymer technology: the current state of the art, *J. Mater. Sci.*, 2007, **42**(9), 2917–2933.



86 Y.-M. Liew, C.-Y. Heah and H. Kamarudin, Structure and properties of clay-based geopolymer cements: a review, *Prog. Mater. Sci.*, 2016, **83**, 595–629.

87 C. Y. Heah, Y. M. Liew, M. M. Al Bakri Abdullah and K. Hussin, Fire resistant properties of geopolymers: a review, *Key Eng. Mater.*, 2015, 39–43.

88 D. Dimas, I. Giannopoulou and D. Panias, Polymerization in sodium silicate solutions: a fundamental process in geopolymerization technology, *J. Mater. Sci.*, 2009, **44**(14), 3719–3730.

89 H. Xu and J. S. van Deventer, The effect of alkali metals on the formation of geopolymeric gels from alkali-feldspars, *Colloids Surf., A*, 2003, **216**(1–3), 27–44.

90 D. Parthiban and D. Vijayan, Study on stress-strain effect of reinforced metakaolin based GPC under compression, *Mater. Today: Proc.*, 2020, **22**, 822–828.

91 Y.-S. Wang, Y. Alrefaei and J.-G. Dai, Silico-aluminophosphate and alkali-aluminosilicate geopolymers: a comparative review, *Front. Mater.*, 2019, **6**, 106.

92 F. Rao and Q. Liu, Geopolymerization and its potential application in mine tailings consolidation: a review, *Miner. Process. Extr. Metall. Rev.*, 2015, **36**(6), 399–409.

93 J. L. Provis, *Modelling the formation of geopolymers*, 2006.

94 Z. Zuhua, Y. Xiao, Z. Huajun and C. Yue, Role of water in the synthesis of calcined kaolin-based geopolymer, *Appl. Clay Sci.*, 2009, **43**(2), 218–223.

95 U. Rattanasak and P. Chindaprasirt, Influence of NaOH solution on the synthesis of fly ash geopolymer, *Miner. Eng.*, 2009, **22**(12), 1073–1078.

96 Y. Liew, H. Kamarudin, A. M. Al Bakri, M. Bnhussain, M. Luqman, I. K. Nizar, C. Ruzaidi and C. Heah, Optimization of solids-to-liquid and alkali activator ratios of calcined kaolin geopolymers powder, *Constr. Build. Mater.*, 2012, **37**, 440–451.

97 H. Wang, H. Li and F. Yan, Synthesis and mechanical properties of metakaolinite-based geopolymer, *Colloids Surf., A*, 2005, **268**(1–3), 1–6.

98 T. Luukkonen, M. Sarkkinen, K. Kemppainen, J. Rämö and U. Lassi, Metakaolin geopolymer characterization and application for ammonium removal from model solutions and landfill leachate, *Appl. Clay Sci.*, 2016, **119**, 266–276.

99 S. S. Ibrahim, A. A. Hagrass, T. R. Boulos, S. I. Youssef, F. I. El-Hossiny and M. R. Moharam, Metakaolin as an active pozzolan for cement that improves its properties and reduces its pollution hazard, *J. Miner. Mater. Charact. Eng.*, 2017, **6**(1), 86–104.

100 Y. Zhang, W. Sun and Z. Li, Hydration process of potassium polysialate (K-PSDS) geopolymer cement, *Adv. Cem. Res.*, 2005, **17**(1), 23–28.

101 M. Kumar, S. K. Saxena and N. B. Singh, Influence of some additives on the properties of fly ash based geopolymer cement mortars, *SN Appl. Sci.*, 2019, **1**(5), 1–12.

102 A. Mustafa Al Bakri, O. A. Abdulkareem, H. Kamarudin, I. Khairul Nizar, R. Abd Razak, Y. Zarina and A. Alida, Microstructure studies on the effect of the alkaline activators of fly ash-based geopolymer at elevated heat treatment temperature, *Appl. Mech. Mater.*, 2013, 342–348.

103 W. Sun, Y.-s. Zhang, W. Lin and Z.-y. Liu, In situ monitoring of the hydration process of K-PS geopolymer cement with ESEM, *Cem. Concr. Res.*, 2004, **34**(6), 935–940.

104 J. Davidovits, Properties of geopolymer cements, in *First international conference on alkaline cements and concretes*, Kiev State Technical University, Kiev, Ukraine, 1994, pp. 131–149.

105 O. Burciaga-Diaz, J. Escalante-Garcia and R. Magallanes-Rivera, Compressive strength and microstructural evolution of metakaolin geopolymers exposed at high temperature, *Revista ALCONPAT*, 2015, **5**(1), 58–72.

106 A. Tawfik, F. Abd-El-Raoof, H. Katsuki, K. Mackenzie and S. Komarneni, Geopolímeros de metakaolin basados en potasio: papel de la relación K/Al y del curado en agua o con vapor a diferentes temperaturas, *Mater. Constr.*, 2016, **66**, e081.

107 A. G. S. Azevedo, K. Strecker, L. A. Barros, L. F. Tonholo and C. T. Lombardi, Effect of curing temperature, activator solution composition and particle size in Brazilian fly-ash based geopolymer production, *Mater. Res.*, 2019, **22**, e20180842.

108 F. Zibouche, H. Kerdjoudj, J.-B. d. E. de Lacaillerie and H. Van Damme, Geopolymers from Algerian metakaolin. Influence of secondary minerals, *Appl. Clay Sci.*, 2009, **43**(3–4), 453–458.

109 P. He, M. Wang, S. Fu, D. Jia, S. Yan, J. Yuan, J. Xu, P. Wang and Y. Zhou, Effects of Si/Al ratio on the structure and properties of metakaolin based geopolymer, *Ceram. Int.*, 2016, **42**(13), 14416–14422.

110 P. Duxson, S. W. Mallicoat, G. C. Lukey, W. M. Kriven and J. S. van Deventer, The effect of alkali and Si/Al ratio on the development of mechanical properties of metakaolin-based geopolymers, *Colloids Surf., A*, 2007, **292**(1), 8–20.

111 A. Palomo, M. T. Blanco-Varela, M. Granizo, F. Puertas, T. Vazquez and M. Grutzeck, Chemical stability of cementitious materials based on metakaolin, *Cem. Concr. Res.*, 1999, **29**(7), 997–1004.

112 M. Criado, A. Fernández-Jiménez, A. De La Torre, M. Aranda and A. Palomo, An XRD study of the effect of the  $\text{SiO}_2/\text{Na}_2\text{O}$  ratio on the alkali activation of fly ash, *Cem. Concr. Res.*, 2007, **37**(5), 671–679.

113 P. Rovnaník, Effect of curing temperature on the development of hard structure of metakaolin-based geopolymer, *Constr. Build. Mater.*, 2010, **24**(7), 1176–1183.

114 E. Najafi Kani and A. Allahverdi, Effects of curing time and temperature on strength development of inorganic polymeric binder based on natural pozzolan, *J. Mater. Sci.*, 2009, **44**(12), 3088–3097.

115 M. Criado, A. Fernández-Jiménez and A. Palomo, Alkali activation of fly ash: effect of the  $\text{SiO}_2/\text{Na}_2\text{O}$  ratio: part I: FTIR study, *Microporous Mesoporous Mater.*, 2007, **106**(1–3), 180–191.

116 Y. Huang, L. Gong, Y. Pan, C. Li, T. Zhou and X. Cheng, Facile construction of the aerogel/geopolymer composite with ultra-low thermal conductivity and high mechanical performance, *RSC Adv.*, 2018, **8**(5), 2350–2356.



117 P. Duxson, J. L. Provis, G. C. Lukey, S. W. Mallicoat, W. M. Kriven and J. S. Van Deventer, Understanding the relationship between geopolymers composition, microstructure and mechanical properties, *Colloids Surf. A*, 2005, **269**(1-3), 47-58.

118 S. Andini, R. Cioffi, F. Colangelo, T. Grieco, F. Montagnaro and L. Santoro, Coal fly ash as raw material for the manufacture of geopolymers-based products, *Waste Manage.*, 2008, **28**(2), 416-423.

119 J. Swanepoel and C. Strydom, Utilisation of fly ash in a geopolymers material, *Appl. Geochem.*, 2002, **17**(8), 1143-1148.

120 M. M. A. B. Abdullah, H. Kamarudin, O. A. Abdulkareem, C. Ruzaidi, R. Razak and N. Mohamed Noor, Optimization of Alkaline Activator/Fly ASH Ratio on the Compressive Strength of Manufacturing Fly ASH-BASED Geopolymer, *Appl. Mech. Mater.*, 2011, **110-116**, 734-739.

121 D. Hardjito, C. C. Cheak and C. L. Ing, Strength and setting times of low calcium fly ash-based geopolymers mortar, *Mod. Appl. Sci.*, 2008, **2**(4), 3-11.

122 S. Pangdaeng, V. Sata, J. Aguiar, F. Pacheco-Torgal and P. Chindaprasirt, Apatite formation on calcined kaolin-white Portland cement geopolymers, *Mater. Sci. Eng. C*, 2015, **51**, 1-6.

123 J. Davidovits, Geopolymer chemistry and properties, in *Proceedings of the 1st International Conference on Geopolymer*, 1988, pp. 25-48.

124 X. Peng, H. Li, Q. Shuai and L. Wang, Fire resistance of alkali activated geopolymers foams produced from metakaolin and Na<sub>2</sub>O<sub>2</sub>, *Materials*, 2020, **13**(3), 535.

125 J. Davidovits, Recent progresses in concretes for nuclear waste and uranium waste containment, *Concr. Int.*, 1994, **16**(12), 53-58.

126 F. Slaty, H. Khoury, H. Rahier and J. Wastiels, Durability of alkali activated cement produced from kaolinitic clay, *Appl. Clay Sci.*, 2015, **104**, 229-237.

127 A. Mehta and R. Siddique, Sulfuric acid resistance of fly ash based geopolymers concrete, *Constr. Build. Mater.*, 2017, **146**, 136-143.

128 N. Sazali, Z. Harun, F. H. Azhar, S. S. Bahri, R. P. N. A. R. Ahmad, R. Hussin and N. Misdan, The effect of various molarity sodium hydroxide (NaOH) on the hydrosodalite formation from synthesis of Johor Kaolin, Malaysia by hydrothermal method, *Mater. Today: Proc.*, 2021, **46**, 2045-2051.

129 A. Sathonsaowaphak, P. Chindaprasirt and K. Pimraksa, Workability and strength of lignite bottom ash geopolymers mortar, *J. Hazard. Mater.*, 2009, **168**(1), 44-50.

130 P. S. Singh, T. Bastow and M. Trigg, Structural studies of geopolymers by <sup>29</sup>Si and <sup>27</sup>Al MAS-NMR, *J. Mater. Sci.*, 2005, **40**(15), 3951-3961.

131 T.-W. Cheng and J. Chiu, Fire-resistant geopolymers produced by granulated blast furnace slag, *Miner. Eng.*, 2003, **16**(3), 205-210.

132 P. Chindaprasirt, T. Chareerat and V. Sirivivatnanon, Workability and strength of coarse high calcium fly ash geopolymers, *Cem. Concr. Compos.*, 2007, **29**(3), 224-229.

133 E. Álvarez-Ayuso, X. Querol, F. Plana, A. Alastuey, N. Moreno, M. Izquierdo, O. Font, T. Moreno, S. Diez and E. Vázquez, Environmental, physical and structural characterisation of geopolymers synthesised from coal (co-) combustion fly ashes, *J. Hazard. Mater.*, 2008, **154**(1-3), 175-183.

134 V. F. F. Barbosa, K. J. Mackenzie and C. Thaumaturgo, Synthesis and characterisation of sodium polysialate inorganic polymer based on alumina and silica, in *Geopolymer'99 International Conference*, France, 1999.

135 K.-L. Lin, H.-S. Shiu, J.-L. Shie, T.-W. Cheng and C.-L. Hwang, Effect of composition on characteristics of thin film transistor liquid crystal display (TFT-LCD) waste glass-metakaolin-based geopolymers, *Constr. Build. Mater.*, 2012, **36**, 501-507.

136 A. Fernández-Jiménez and A. Palomo, Factors affecting early compressive strength of alkali activated fly ash (OPC-free) concrete, *Mater. Constr.*, 2007, **57**(287), 7-22.

137 C. Shi, A. F. Jiménez and A. Palomo, New cements for the 21st century: the pursuit of an alternative to Portland cement, *Cem. Concr. Res.*, 2011, **41**(7), 750-763.

138 F. Pelisser, *et al.*, Micromechanical characterization of metakaolin-based geopolymers, *Constr. Build. Mater.*, 2013, **49**, 547-553.

139 A. Poowancum and S. Horpibulsuk, Development of low cost geopolymers from calcined sedimentary clay, in *Calcined Clays for Sustainable Concrete*, Springer, 2015, pp. 359-364.

140 F. Pelisser, E. Guerrino, M. Menger, M. Michel and J. Labrincha, Micromechanical characterization of metakaolin-based geopolymers, *Constr. Build. Mater.*, 2013, **49**, 547-553.

141 A. Lăzărescu, C. Mircea, H. Szilagyi and C. Baeră, Mechanical properties of alkali activated geopolymers paste using different Romanian fly ash sources-experimental results, in *MATEC Web of Conferences*, EDP Sciences, 2019, p. 11001.

142 D. Hardjito and B. V. Rangan, *Development and properties of low-calcium fly ash-based geopolymers concrete*, 2005.

143 D. Hardjito, S. E. Wallah, D. Sumajouw and B. Rangan, *Properties of geopolymers concrete with fly ash as source material: effect of mixture composition*, Special Publication, 2004, vol. 222, pp. 109-118.

144 G. Li and X. Wu, Influence of fly ash and its mean particle size on certain engineering properties of cement composite mortars, *Cem. Concr. Res.*, 2005, **35**(6), 1128-1134.

145 C. F. Ferraris, Measurement of the rheological properties of high performance concrete: state of the art report, *J. Res. Natl. Inst. Stand. Technol.*, 1999, **104**(5), 461.

146 J. Davidovits, *Mineral Polymers and Methods of Making Them*, US Pat. 4,349,386, 1982.

147 H. Wang, H. Wu, Z. Xing, R. Wang and S. Dai, The Effect of Various Si/Al, Na/Al Molar Ratios and Free Water on Micromorphology and Macro-Strength of Metakaolin-Based Geopolymer, *Materials*, 2021, **14**(14), 3845.

148 C. Shi, D. Roy and P. Krivenko, *Alkali-activated cements and concretes*, CRC Press, 2003.



149 J. Provis and J. Van Deventer, Geopolymerisation kinetics. 2. Reaction kinetic modelling, *Chem. Eng. Sci.*, 2007, **62**(9), 2318–2329.

150 J. L. Provis and J. S. Van Deventer, Geopolymerisation kinetics. 1. In situ energy-dispersive X-ray diffractometry, *Chem. Eng. Sci.*, 2007, **62**(9), 2309–2317.

151 M. Lizcano, A. Gonzalez, S. Basu, K. Lozano and M. Radovic, Effects of water content and chemical composition on structural properties of alkaline activated metakaolin-based geopolymers, *J. Am. Ceram. Soc.*, 2012, **95**(7), 2169–2177.

152 R. A. Fletcher, K. J. MacKenzie, C. L. Nicholson and S. Shimada, The composition range of aluminosilicate geopolymers, *J. Eur. Ceram. Soc.*, 2005, **25**(9), 1471–1477.

153 G. Nasab, F. Golestanifard and K. MacKenzie, The effect of the  $\text{SiO}_2/\text{Na}_2\text{O}$  ratio in the structural modification of metakaolin-based geopolymers studied by XRD, FTIR and MAS-NMR, *Journal of Ceramic Science and Technology*, 2014, **5**(3), 185–191.

154 H. Rahier, W. Simons, B. Van Mele and M. Biesemans, Low-temperature synthesized aluminosilicate glasses: part III influence of the composition of the silicate solution on production, structure and properties, *J. Mater. Sci.*, 1997, **32**(9), 2237–2247.

155 J. L. Provis, C. Z. Yong, P. Duxson and J. S. van Deventer, Correlating mechanical and thermal properties of sodium silicate-fly ash geopolymers, *Colloids Surf., A*, 2009, **336**(1–3), 57–63.

156 B. Latella, D. Perera, D. Durce, E. Mehrtens and J. Davis, Mechanical properties of metakaolin-based geopolymers with molar ratios of  $\text{Si}/\text{Al} \approx 2$  and  $\text{Na}/\text{Al} \approx 1$ , *J. Mater. Sci.*, 2008, **43**(8), 2693–2699.

157 A. Kamalloo, Y. Ganjkhlanlou, S. H. Aboutalebi and H. Nouranian, *Modeling of compressive strength of metakaolin based geopolymers by the use of artificial neural network*, 2010.

158 R. Pouhet, *Formulation and durability of metakaolin-based geopolymers*, Université Paul Sabatier-Toulouse III, 2015.

159 A. Lăzărescu, H. Szilagyi, C. Baeră and A. Ioani, The effect of alkaline activator ratio on the compressive strength of fly ash-based geopolymer paste, in *IOP conference series: materials science and engineering*, IOP Publishing, 2017, p. 012064.

160 D. Perera, O. Uchida, E. Vance and K. Finnie, Influence of curing schedule on the integrity of geopolymers, *J. Mater. Sci.*, 2007, **42**(9), 3099–3106.

161 C. Kuenzel, L. J. Vandeperre, S. Donatello, A. R. Boccaccini and C. Cheeseman, Ambient temperature drying shrinkage and cracking in metakaolin-based geopolymers, *J. Am. Ceram. Soc.*, 2012, **95**(10), 3270–3277.

162 J. He, Y. Jie, J. Zhang, Y. Yu and G. Zhang, Synthesis and characterization of red mud and rice husk ash-based geopolymer composites, *Cem. Concr. Compos.*, 2013, **37**, 108–118.

163 B.-h. Mo, H. Zhu, X.-m. Cui, Y. He and S.-y. Gong, Effect of curing temperature on geopolymerization of metakaolin-based geopolymers, *Appl. Clay Sci.*, 2014, **99**, 144–148.

164 N. Wielgus, M. Górski and J. Kubica, Discarded cathode ray tube glass as an alternative for aggregate in a metakaolin-based geopolymer, *Sustainability*, 2021, **13**(2), 479.

165 M. Khalil and E. Merz, Immobilization of intermediate-level wastes in geopolymers, *J. Nucl. Mater.*, 1994, **211**(2), 141–148.

166 M. Tashima, L. Soriano, M. Borrachero, J. Monzó and J. Payá, Effect of curing time on microstructure and mechanical strength development of alkali activated binders based on vitreous calcium aluminosilicate (VCAS), *Bull. Mater. Sci.*, 2013, **36**(2), 245–249.

167 Y. Wang, S. Hu and Z. He, Mechanical and fracture properties of fly ash geopolymer concrete additive with calcium aluminate cement, *Materials*, 2019, **12**(18), 2982.

168 T. Kovářík, P. Franče, J. Šesták, D. Rieger, P. Bělský, J. Kadlec and P. Roubíček, A novel approach to polyaluminosilicates curing process using electric boosting and temperature profile investigation by DSC, *J. Therm. Anal. Calorim.*, 2015, **121**(1), 517–524.

169 H. Kim and Y. Kim, Relationship between compressive strength of geo-polymers and pre-curing conditions, *Appl. Microsc.*, 2013, **43**(4), 155–163.

170 T.-A. Chen, Mechanical Properties of Glass-Based Geopolymers Affected by Activator and Curing Conditions under Optimal Aging Conditions, *Crystals*, 2021, **11**(5), 502.

171 B. Satpute Manesh, R. Wakchaure Madhukar and V. Patankar Subhash, Effect of duration and temperature of curing on compressive strength of geopolymer concrete, *International Journal of Engineering and Innovative Technology*, 2012, **1**, 152–155.

172 B. Kim and S. Lee, Review on characteristics of metakaolin-based geopolymer and fast setting, *J. Korean Ceram. Soc.*, 2020, **57**(4), 368–377.

173 J. Davidovits and M. Davidovics, Geopolymer: ultra-high temperature tooling material for the manufacture of advanced composites, *How Concept Becomes Reality*, 1991, **36**, 1939–1949.

174 C. Kuenzel, L. Grover, L. Vandeperre, A. Boccaccini and C. Cheeseman, Production of nepheline/quartz ceramics from geopolymer mortars, *J. Eur. Ceram. Soc.*, 2013, **33**(2), 251–258.

175 N. A. Jaya, M. M. Al Bakri Abdullah and R. Ahmad, Reviews on clay geopolymer ceramic using powder metallurgy method, in *Materials Science Forum*, Trans Tech Publications, 2015, pp. 81–87.

176 K. Pimraksa, P. Chindaprasirt, A. Rungchet, K. Sagoe-Crentsil and T. Sato, Lightweight geopolymer made of highly porous siliceous materials with various  $\text{Na}_2\text{O}/\text{Al}_2\text{O}_3$  and  $\text{SiO}_2/\text{Al}_2\text{O}_3$  ratios, *Mater. Sci. Eng., A*, 2011, **528**(21), 6616–6623.

177 R. A. Aguilar, O. B. Díaz and J. E. García, Lightweight concretes of activated metakaolin-fly ash binders, with blast furnace slag aggregates, *Constr. Build. Mater.*, 2010, **24**(7), 1166–1175.

178 E. Prud'Homme, P. Michaud, E. Joussein, C. Peyratout, A. Smith and S. Rossignol, In situ inorganic foams



prepared from various clays at low temperature, *Appl. Clay Sci.*, 2011, **51**(1–2), 15–22.

179 Z. Zhang, K. Wang, B. Mo, X. Li and X. Cui, Preparation and characterization of a reflective and heat insulative coating based on geopolymers, *Energy and Buildings*, 2015, **87**, 220–225.

180 J. Temuujin, A. Minjigmaa, W. Rickard, M. Lee, I. Williams and A. Van Riessen, Preparation of metakaolin based geopolymer coatings on metal substrates as thermal barriers, *Appl. Clay Sci.*, 2009, **46**(3), 265–270.

181 H. Y. Zhang, V. Kodur, S. L. Qi, L. Cao and B. Wu, Development of metakaolin-fly ash based geopolymers for fire resistance applications, *Constr. Build. Mater.*, 2014, **55**, 38–45.

182 J. Henon, A. Alzina, J. Absi, D. S. Smith and S. Rossignol, Potassium geopolymer foams made with silica fume pore forming agent for thermal insulation, *J. Porous Mater.*, 2013, **20**(1), 37–46.

183 E. Kamseu, B. Ceron, H. Tobias, E. Leonelli, M. Bignozzi, A. Muscio and A. Libbra, Insulating behavior of metakaolin-based geopolymer materials assess with heat flux meter and laser flash techniques, *J. Therm. Anal. Calorim.*, 2012, **108**(3), 1189–1199.

184 J. Temuujin, A. Minjigmaa, W. Rickard and A. Van Riessen, Thermal properties of spray-coated geopolymer-type compositions, *J. Therm. Anal. Calorim.*, 2012, **107**(1), 287–292.

185 P. Sukontasukkul, N. Nontiyutsirikul, S. Songpiriyakul, K. Sakai and P. Chindaprasirt, Use of phase change material to improve thermal properties of lightweight geopolymer panel, *Mater. Struct.*, 2016, **49**(11), 4637–4645.

186 C. Ponzoni, I. Lancellotti, L. Barbieri, A. Spinella, M. L. Saladino, D. C. Martino, E. Caponetti, F. Armetta and C. Leonelli, Chromium liquid waste inertization in an inorganic alkali activated matrix: leaching and NMR multinuclear approach, *J. Hazard. Mater.*, 2015, **286**, 474–483.

187 D.-L. Chequer and F. Frizon, Impact of sulfate and nitrate incorporation on potassium-and sodium-based geopolymers: geopolymerization and materials properties, *J. Mater. Sci.*, 2011, **46**(17), 5657–5664.

188 K. Okada, A. Ooyama, T. Isobe, Y. Kameshima, A. Nakajima and K. J. MacKenzie, Water retention properties of porous geopolymers for use in cooling applications, *J. Eur. Ceram. Soc.*, 2009, **29**(10), 1917–1923.

189 F. Pacheco-Torgal, Z. Abdollahnejad, S. Miraldo, S. Baklouti and Y. Ding, An overview on the potential of geopolymers for concrete infrastructure rehabilitation, *Constr. Build. Mater.*, 2012, **36**, 1053–1058.

190 C. F. Geraldes, A. M. Lima, J. Delgado-Rodrigues, J. M. Mimoso and S. R. Pereira, Geopolymers as potential repair material in tiles conservation, *Appl. Phys. A: Mater. Sci. Process.*, 2016, **122**(3), 1–10.

191 T.-C. Hung, J.-S. Huang, Y.-W. Wang and K.-Y. Lin, Inorganic polymeric foam as a sound absorbing and insulating material, *Constr. Build. Mater.*, 2014, **50**, 328–334.

192 P. Sturm, S. Greiser, G. Gluth, C. Jäger and H. Brouwers, Degree of reaction and phase content of silica-based one-part geopolymers investigated using chemical and NMR spectroscopic methods, *J. Mater. Sci.*, 2015, **50**(20), 6768–6778.

193 E. Jämstorp, J. Forsgren, S. Bredenberg, H. Engqvist and M. Strømme, Mechanically strong geopolymers offer new possibilities in treatment of chronic pain, *J. Controlled Release*, 2010, **146**(3), 370–377.

194 B. Cai, H. Engqvist and S. Bredenberg, Evaluation of the resistance of a geopolymer-based drug delivery system to tampering, *Int. J. Pharm.*, 2014, **465**(1–2), 169–174.

